34]. Although we cannot exclude the possibility that the cells die as a result of redox stress itself, the residual ALS neurons expressing redox system up-regulation are thought to maintain their viability by protecting themselves from potentially destructive ROSs and by controlling the intraneuronal redox system [1, 5, 10, 14, 34, 39]. A similar up-regulation mechanism for hepatocyte growth factor (HGF, a novel neurotrophic factor) and its receptor (c-Met) also occurs in the SALS and SOD1-mutated FALS patients [22]. Considering that in the animal experiment, overexpression of HGF attenuates motor neuron death and prolongs the life span of G1L-G93A mice [37], motor neurons showing up-regulation of the HGF/c-Met cell-survival system, which is normally present in neurons, are thought to show enhanced cell survival in the presence of ALS stress in humans [22]. Although we cannot readily compare the neurotrophic factor with the redox system, our finding leads us to the conclusion that the residual ALS neurons showing redox system up-regulation would be less susceptible to ALS stress and can protect themselves from ALS neuronal death. Taken together with the fact that Prxll functions not only as a member of the redox system but also as a molecular chaperone [18], the residual ALS neurons overexpresing Prxll/GPxl might have developed to possess simultaneously both the enhanced antioxidant enzyme defense mechanism as a highly-evolved redox system, and the amplified sophisticated system for coping with misfolded proteins, such as mutant SOD1 or unknown pathogenetic proteins leading to SALS. Thus, residual ALS neurons overexpressing redox system-related enzymes could protect themselves from ALS stress. However, it is not thought possible for residual ALS neurons under long-term ALS stress to keep on inducing redox system-related enzymes. Therefore, as ALS progresses, the ability of residual neurons to up-regulate the redox system diminishes, and finally they become even unable to maintain the redox system itself. In other words, ALS neurons showing redox system up-regulation might show enhanced cell survival in the presence of ALS stress. In contrast, breakdown of the redox system in ALS motor neurons that are barely viable would result in cell death, and many residual motor neurons that are unable to coexpress Prxll/GPxl would ultimately become moribund.

Our data may lead to the development of a new therapy based on redox system up-regulation for the treatment of ALS, which for over 130 years has had an unknown etiology. It remains to be determined whether this redox system up-regulation is a direct or an indirect effect based on the pathogenesis of ALS itself, or whether this redox system up-regulation plays a primary or a secondary role in attenuating ALS-related neuronal death.

Acknowledgements This study was supported in part by a Research Grant on Measures for Intractable Diseases from the Ministry of Health, Labour and Welfare of Japan (S.K. and Y.I.); a Research Grant (2004) from the Faculty of Medicine, Tottori University (S.K.); a Grant-in-Aid for Scientific Research in Priority Area (T.N.) and a Grant-in-Aid for Scientific Research (Y.A.) from the Ministry of Education Culture, Sports, Science and Technology of Japan.

References

1. Andoh T, Chiueh CC, Chock PB (2003) Cyclic GMP-dependent protein kinase regulates the expression of thioredoxin and thioredoxin peroxidase-1 during hormesis in response to oxidative stress-induced apoptosis. J Biol Chem 278:885–890
2. Asayama K, Burr IM (1984) Joint purification of mangano and cuprozinc superoxide dismutases from a single source: a simplified method. Anal Biochem 136:336–339
3. Asayama K, Yokota S, Dobashi K, Hayashibe H, Kawaoi A, Nakazawa S (1994) Purification and immunoelectron microscopic localization of cellular glutathione peroxidase in rat hepatocytes: quantitative analysis by postembedding method. Histochemistry 102:213–219
4. Berggren MI, Husbeck B, Samulitis B, Baker AF, Gallegos A, Powis G (2001) Thioredoxin peroxidase-1 (peroxiredoxin-1) is increased in thioredoxin-1 transfected cells and results in enhanced protection against apoptosis caused by hydrogen peroxide but not by other agents including dexamethasone, etoposide, and doxorubicin. Arch Biochem Biophys 392:103–109
5. Biteau B, Labarre J, Toledano MB (2003) ATP-dependent reduction of cysteine-sulphinic acid by *S. cerevisiae* sulphiredoxin. Nature 425:980–984
6. Chae HZ, Kim IH, Kim K, Rhee SG (1993) Cloning, sequencing, and mutation of thiol-specific antioxidant gene of *Saccharomyces cerevisiae*. J Biol Chem 268:16815–16821
7. Chae HZ, Chung SJ, Rhee SG (1994) Thioredoxin-dependent peroxide reductase from yeast. J Biol Chem 269:27670–27678
8. Chae HZ, Robison K, Poole LB, Church G, Storz G, Rhee SG (1994) Cloning and sequencing of thiol-specific antioxidant from mammalian brain: alkyl hydroperoxide reductase and thiol-specific antioxidant define a large family of antioxidant enzymes. Proc Natl Acad Sci USA 91:7017–7021
9. Chang TS, Jeong W, Choi SY, Yu S, Kang SW, Rhee SG (2002) Regulation of peroxiredoxin I activity by cdc2-mediated phosphorylation. J Biol Chem 277:25370–25376
10. Chang TS, Jeong W, Woo HA, Lee SM, Park S, Rhee SG (2004) Characterization of mammalian sulfiredoxin and its reactivation of hyperoxidized peroxiredoxin through reduction of cysteine sulfinic acid in the active site to cysteine. J Biol Chem 279:50994–51001
11. Charcot JM, Joffroy A (1869) Deux cas d'atrophie musculaire progressive avec lésions de la substance grise et des faisceaux antéro-latéraux de la moelle épinière. Arch Physiol (Paris) 2:744–760
12. De Haan JB, Bladier C, Griffiths P, Kelner M, O'Shea RD, Cheung NS, Bronson RT, Silvestro MJ, Wild S, Zheng SS, Beart PM, Hertzog PJ, Kola I (1998) Mice with a homozygous null mutation for the most abundant glutathione peroxidase, Gpx1, show increased susceptibility to the oxidative stress-inducing agents paraquat and hydrogen peroxide. J Biol Chem 273:22528–22536
13. Fridovich I (1986) Superoxide dismutases. Adv Enzymol Relat Areas Mol Biol 58:61–97
14. Georgiou G, Masip L (2003) An overoxidation journey with a return ticket. Science 300:592–594
15. Hirotsu S, Abe Y, Nagahara N, Hori H, Nishino T, Okada K, Hakoshima T (1999) Crystallographic characterization of a stress-induced multifunctional protein, rat HBP-23. J Struct Biol 126:80–83
16. Hirotsu S, Abe Y, Okada K, Nagahara N, Hori H, Nishino T, Hakoshima T (1999) Crystal structure of a multifunctional 2-Cys peroxiredoxin heme-binding protein 23 kDa/proliferation-associated gene product. Proc Natl Acad Sci USA 96:12333–12338

17. Ichimiya S, Davis JG, O'Rourke DM, Katsumata M, Greene MI (1997) Murine thioredoxin peroxidase delays neuronal apoptosis and is expressed in areas of the brain most susceptible to hypoxic and ischemic injury. DNA Cell Biol 16:311–321
18. Jang HH, Lee KO, Chi YH, Jung BG, Park SK, Park JH, Lee JR, Lee SS, Moon JC, Yun JW, Choi YO, Kim WY, Kang JS, Cheong GW, Yun DJ, Rhee SG, Cho MJ, Lee SY (2004) Two enzymes in one; two yeast peroxiredoxins display oxidative stress-dependent switching from a peroxidase to a molecular chaperone function. Cell 117:625–635
19. Jin D-Y, Chae HZ, Rhee SG, Jeang K-T (1997) Regulatory role for a novel human thioredoxin peroxidase in NF-kappaB activation. J Biol Chem 272:30952–30961
20. Kato S, Shimoda M, Watanabe Y, Nakashima K, Takahashi K, Ohama E (1996) Familial amyotrophic lateral sclerosis with a two base pair deletion in superoxide dismutase 1 gene: multisystem degeneration with intracytoplasmic hyaline inclusions in astrocytes. J Neuropathol Exp Neurol 55:1089–1101
21. Kato S, Hayashi H, Nakashima K, Nanba E, Kato M, Hirano A, Nakano I, Asayama K, Ohama E (1997) Pathological characterization of astrocytic hyaline inclusions in familial amyotrophic lateral sclerosis. Am J Pathol 151:611–620
22. Kato S, Funakoshi H, Nakamura T, Kato M, Nakano I, Hirano A, Ohama E (2003) Expression of hepatocyte growth factor and c-Met in the anterior horn cells of the spinal cord in the patients with amyotrophic lateral sclerosis (ALS): immunohistochemical studies on sporadic ALS and familial ALS with superoxide dismutase 1 gene mutation. Acta Neuropathol 106:112–120
23. Kato S, Shaw P, Wood-Allum C, Leigh PN, Show C (2003) Amyotrophic lateral sclerosis. In: Dickson D (ed) Nerodegeneration: the molecular pathology of dementia and movement disorders. ISN Neuropath Press, Basel, pp 350–368
24. Kato S, Saeki Y, Aoki M, Nagai M, Ishigaki A, Itoyama Y, Kato M, Asayama K, Awaya A, Hirano A, Ohama E (2004) Histological evidence of redox system breakdown caused by superoxide dismutase 1 (SOD1) aggregation is common to SOD1-mutated motor neurons in humans and animal models. Acta Neuropathol 107:149–158
25. Kato T, Hirano A, Kurland LT (1987) Asymmetric involvement of the spinal cord involving both large and small anterior horn cells in a case of familial amyotrophic lateral sclerosis. Clin Neuropathol 6:67–70
26. Koo KH, Lee S, Jeong SY, Kim ET, Kim HJ, Kim K, Song K, Chae HZ (2002) Regulation of thioredoxin peroxidase activity by c-terminal truncation. Arch Biochem Biophys 397:312–318
27. Kosower NS, Kosower EM (1978) The glutathione status of cells. Int Rev Cytol 54:109–160
28. Kurland LT, Mulder DW (1955) Epidemiologic investigations of amyotrophic lateral sclerosis. II. Familial aggregations indicative of dominant inheritance. Neurology 5:182–196, 249–268
29. Matsumoto A, Okado A, Fujii T, Fujii J, Egashira M, Niikawa N, Taniguchi N (1999) Cloning of the peroxiredoxin gene family in rats and characterization of the fourth member. FEBS Lett 443:246–250
30. Meister A, Anderson ME (1983) Glutathione. Annu Rev Biochem 52:711–760
31. Mu ZM, Yin XY, Prochownik EV (2002) Pag, a putative tumor suppressor, interacts with the myc box II domain of c-myc and selectively alters its biological function and target gene expression. J Biol Chem 277:43175–43184
32. Nagai M, Aoki M, Miyoshi I, Kato M, Pasinelli P, Kasai N, Brown RH Jr, Itoyama Y (2001) Rats expressing human cytosolic copper-zinc superoxide dismutase transgenes with amyotrophic lateral sclerosis: associated mutations develop motor neuron disease. J Neurosci 21:9246–9254
33. Nakano I, Hirano A, Kurland LT, Mulder DW, Holley PW, Saccomanno G (1984) Familial amyotrophic lateral sclerosis. Neuropathology of two brothers in American "C" family. Neurol Med (Tokyo) 20:458–471
34. Neumann CA, Krause DS, Carman CV, Das S, Dubey DP, Abraham JL, Bronson RT, Fujiwara Y, Orkin SH, Van Etten RA (2003) Essential role for the peroxiredoxin prdx1 in erythrocyte antioxidant defence and tumour suppression. Nature 424:561–565
35. Sen CK, Packer L (1996) Antioxidant and redox regulation of gene transcription. FASEB J 10:709–720
36. Shibata N, Hirano A, Kobayashi M, Siddique T, Deng HX, Hung WY, Kato T, Asayama K (1996) Intense superoxide dismutase-1 immunoreactivity in intracytoplasmic hyaline inclusions of familial amyotrophic lateral sclerosis with posterior column involvement. J Neuropathol Exp Neurol 55:481–490
37. Sun W, Funakoshi H, Nakamura T (2002) Overexpression of HGF retards disease progression and prolongs life span in a transgenic mouse model of ALS. J Neurosci 22:6537–6548
38. Takahashi K, Nakamura H, Okada E (1972) Hereditary amyotrophic lateral sclerosis. Histochemical and electron microscopic study of hyaline inclusions in motor neurons. Arch Neurol 27:292–299
39. Wood ZA, Poole LB, Karplus PA (2003) Peroxiredoxin evolution and the regulation of hydrogen peroxide signaling. Science 300:650–653

Available online at www.sciencedirect.com
SCIENCE DIRECT
ELSEVIER
Biochemical and Biophysical Research Communications 343 (2006) 719–730
BBRC
www.elsevier.com/locate/ybbrc

Alteration of familial ALS-linked mutant SOD1 solubility with disease progression: Its modulation by the proteasome and Hsp70

Shingo Koyama [a], Shigeki Arawaka [a,*], Ren Chang-Hong [a], Manabu Wada [a], Toru Kawanami [a], Keiji Kurita [a], Masaaki Kato [b], Makiko Nagai [b], Masashi Aoki [b], Yasuto Itoyama [b], Gen Sobue [c], Pak H. Chan [d], Takeo Kato [a]

[a] *Department of Neurology, Hematology, Metabolism, Endocrinology and Diabetology, Yamagata University School of Medicine, 2-2-2 Iida-nishi, Yamagata 990-9585, Japan*
[b] *Department of Neurology, Tohoku University Graduate School of Medicine, Sendai, Japan*
[c] *Department of Neurology, Nagoya University Graduate School of Medicine, Nagoya, Japan*
[d] *Department of Neurosurgery, Stanford University School of Medicine, Stanford, CA, USA*

Received 9 February 2006
Available online 9 March 2006

Abstract

Accumulation of misfolded Cu/Zn superoxide dismutase (SOD1) occurs in patients with a subgroup of familial amyotrophic lateral sclerosis (fALS). To identify the conversion of SOD1 from a normally soluble form to insoluble aggregates, we investigated the change of SOD1 solubility with aging in fALS-linked H46R SOD1 transgenic mice. Mutant SOD1 specifically altered to insoluble forms, which were sequentially separated into Triton X-100-insoluble/sodium dodecyl sulfate (SDS)-soluble and SDS-insoluble/formic acid-soluble species. In spinal cords, the levels of SDS-dissociable soluble SOD1 monomers and SDS-stable soluble dimers were significantly elevated before motor dysfunction onset. In COS-7 cells expressing H46R SOD1, treatment with proteasome inhibitors recapitulated the alteration of SOD1 solubility in transgenic mice. In contrast, overexpression of Hsp70 reduced accumulation of mutant-specific insoluble SOD1. SDS-soluble low molecular weight species of H46R SOD1 may appear as early misfolded intermediates when their concentration exceeds the capacity of the proteasome and molecular chaperones.

Keywords: Amyotrophic lateral sclerosis; Cu/Zn superoxide dismutase; Heat shock protein; Proteasome; Oligomer

Amyotrophic lateral sclerosis (ALS) is a neurodegenerative disorder characterized by the degeneration of both upper and lower motor neurons, leading to progressive paralysis. Of all ALS cases, ~90% are sporadic and ~10% are familial; ~20% of familial ALS (fALS) cases are associated with dominantly inherited mutations in the gene encoding Cu/Zn superoxide dismutase (SOD1) [1–3]. SOD1 is a major antioxidant enzyme located predominantly in the cytosol, nucleus, and mitochondrial intermembrane space of eukaryotic cells [4]. The biological active enzyme forms a 32-kDa homodimer and contains one copper-binding site and one zinc-binding site, as well as a disulfide bond in each of its two subunits. SOD1-linked fALS was initially suspected to result from oxidative damage caused by diminished SOD1 activity, but SOD1-null mice show no motor neuron disease [5], and transgenic mice overexpressing human mutant SOD1 have a phenotype that is closely similar to patients with fALS, irrespective of their normal or elevated levels of SOD1 activity [6–9]. This evidence indicates that SOD1-linked fALS occurs due to a toxic gain-of-function of mutant SOD1 but not due to a lowering of its activity [6].

Deposition of proteinaceous inclusions of SOD1 in motor neurons is a characteristic hallmark of patients with fALS [10–12]. Cellular and animal models have shown that overexpression of mutant SOD1 can cause loss of motor

* Corresponding author. Fax: +81 23 628 5318.
E-mail address: arawaka@med.id.yamagata-u.ac.jp (S. Arawaka).

0006-291X/$ - see front matter © 2006 Elsevier Inc. All rights reserved.
doi:10.1016/j.bbrc.2006.02.170

neurons with the formation of SOD1-positive inclusions [12–15] and high-molecular-weight (HMW) SOD1 complexes [12,16–19], supporting the hypothesis that the abnormal accumulation of SOD1 aggregates may play a role in the pathogenesis of fALS. Concerning the formation of SOD1 aggregates, several reports have described a close association with the proteasome and heat shock proteins (Hsps). In cells overexpressing mutant SOD1, inhibition of the proteasome activity resulted in the accumulation of insoluble SOD1 protein and the formation of HMW insoluble complexes [16,17,19–22]. On the other hand, Bruening et al. [23] reported that overexpression of Hsp70 reduced aggregate formation and prolonged cellular viability in cells expressing mutant SOD1. These data imply that the conversion of SOD1 from an inherently soluble form to an aggregated species is promoted by insufficiency of the proteasome and/or molecular chaperones, which suppress the accumulation of misfolded proteins. However, the formation of protein aggregation is a complex process, which contains several kinds of misfolded intermediates to form amorphous aggregates and fibrils [24]. There is only a little basic information on how mutant SOD1 undergoes the complex process in relation to the system of proteasome and Hsps.

In the present study, we investigated the alteration of SOD1 solubility with aging in fALS-linked mutant H46R SOD1 transgenic mice. We also examined its change in mutant SOD1 expressed cells by treatment with proteasome inhibitors. Furthermore, using cells co-expressing mutant SOD1 and Hsp70, we characterized an insoluble SOD1 species influenced by Hsp70 as misfolded proteins. Here we show that SDS-dissociable soluble monomers and SDS-stable soluble dimers of H46R SOD1 appear as early misfolded intermediates in the formation of highly insoluble aggregates, and their levels are coordinately mediated by the proteasome activity and Hsp function.

Materials and methods

Materials. We used the following antibodies: polyclonal human SOD1 antibody (SOD1-100, diluted 0.1 μg/ml, Victoria, BC, Canada); monoclonal antibody against GST-fused full-length human SOD1 protein that specifically binds to human SOD1 (diluted 0.2 μg/ml, MBL, Nagoya, Japan); polyclonal Hsp70 antibody (SPA-757, diluted 1:30,000 for Western blotting, diluted 1:1000 for immunohistochemistry, Stressgen); polyclonal Hsp40 antibody (SPA-400 diluted 1:10,000 for Western blotting, diluted 1:500 for immunohistochemistry, Stressgen). Wild-type SOD1 cDNA fused with an FLAG tag at C-terminus of SOD1 (SOD1-FLAG) was subcloned into either pcDNA3.1 (Invitrogen, Carlsbad, CA, USA) or pEF-BOS vector [20]. Mutant H46R and G93A SOD1 cDNAs were generated by site-directed mutagenesis, and their sequences were confirmed by DNA sequencing. pCMV-Hsp70 and pRC-Hsp40 were described previously [25,26].

Cell culture and transfection. COS-7 and SH-SY5Y cells were grown in Dulbecco's modified Eagle's medium (DMEM, Invitrogen) and a mixture of DMEM and Ham's F-12, respectively, supplemented with 10% fetal bovine serum. SOD1 cDNAs were transfected into cells using Lipofectamine Plus reagents (Invitrogen), according to the manufacturer's protocols [27]. Cultured cells were harvested 48 h after transfection for experiments. For inhibition of the proteasome activity, either MG132 or lactacystin (Sigma, St. Louis, MO, USA) in indicated concentrations was added to cells 24 h after transfection and then cells were further incubated for 24 h. In experiments using Hsp chaperones, either Hsp70 or Hsp40 cDNA was co-transfected with H46R SOD1-FLAG pEF-BOS to COS-7 cells (at a molar ratio of 4:1).

Transgenic mice. Transgenic mouse lines expressing fALS-linked H46R SOD1 under the control of inherent human SOD1 promoter were maintained as hemizygotes by mating with B6/SJF1 as previously described [28]. The transgenic mice expressing wild-type human SOD1 were also kindly supplied by Dr. PH. Chan (Stanford University, Stanford, CA, USA) and maintained as hemizygotes [29]. All of the mouse experiments followed the Guidelines for Animal Experiments of Yamagata University School of Medicine.

Protein fractionation and Western blotting. Protein fractionation of whole mouse spinal cords was performed according to published protocols [30,31] with a slight modification (see Fig. 1A). Whole mouse spinal cords were homogenized by 15 up-and-down strokes with a Teflon homogenizer in 1:3 (wt/vol) phosphate-buffered saline (PBS; 100 mM phosphate, pH 7.4, 150 mM NaCl, and protease inhibitor cocktail (Roche Diagnostics, Mannheim, Germany)). The homogenate was centrifuged at 100,000×*g* for 20 min at 4 °C, and the resultant supernatant was collected as the PBS-soluble fraction. The pellet was rinsed three times with PBS and was extracted by sonication in 1% Triton X-100 (TX)/PBS. After centrifugation at 100,000×*g* for 20 min at 4 °C, the supernatant was designated as the TX-soluble fraction. The pellet was washed three times with 1% TX/PBS and extracted by sonication in 5% SDS/PBS. The extract was incubated at room temperature for 30 min and centrifuged at 100,000×*g* for 20 min at 20 °C. The supernatant was designated as the SDS-soluble fraction. After rinsing and centrifugating three times in 5% SDS/PBS, the resultant pellet was extracted by sonication in 8 M urea/PBS. After centrifugation at 100,000×*g* for 20 min at 20 °C, the supernatant was designated as the urea-soluble fraction. The pellet was rinsed once with 8 M urea/PBS and extracted by sonication in 88% formic acid (FA). After centrifugation at 100,000×*g* for 20 min at 20 °C, the supernatant was designated as the FA-soluble fraction. FA was evaporated by SpeedVac (Savant, Farmingdale, NY, USA). After washing the dried pellet with distilled water and lyophilizing it again, the resulting pellet was resuspended by sonication in Laemmli's sample buffer containing 2% SDS and 100 mM dithiothreitol and then boiled for 5 min. The protein concentrations of the PBS-soluble, TX-soluble, SDS-soluble, and urea-soluble fractions were measured by a BCA protein assay (Pierce, Rockford, IL, USA). Cultured cell pellets were fractionated by the same protocol described above until the preparation of the SDS-soluble fraction. The SDS-insoluble pellet was resuspended by sonication in Laemmli's sample buffer and boiled for 5 min. The suspension was designated as the SDS-insoluble fraction.

We performed Western blotting as described previously [27]. All protein samples were boiled for 5 min in Laemmli's sample buffer containing 100 mM dithiothreitol. Ten micrograms of protein from each of the PBS-soluble, TX-soluble, SDS-soluble, and urea-soluble fractions, and equal aliquots of the FA-soluble fraction were loaded on 15% polyacrylamide gels. The relative intensities of detected bands were scanned and quantified with the Scion image program, version 4.02 (Scion Corp., Frederick, MD, USA). Statistical analysis for comparison of groups was performed by ANOVA with Fisher's probability of least significant difference (PLSD) post hoc test for significance using the Statview software version 5 (SAS Institute Inc, Cary, NC, USA).

Immunohistochemistry. The mice, anesthetized with diethyl ether, were sacrificed by transcardial perfusion with 0.9% sodium chloride followed by 4% paraformaldehyde in PBS. The spinal cord was quickly removed, post-fixed with the above solution, and then embedded in paraffin. After deparaffinizing, sections (4-μm thickness) of the lumbar spinal cord (L_{4-5}) were incubated with 0.3% hydrogen peroxide for 10 min and then with 10% normal goat serum for 30 min. The sections were incubated with the primary antibodies, and they reacted with the appropriate biotinylated secondary antibodies, followed by an avidin-biotin-peroxidase complex (Vector, Burlingame, CA, USA). Color was developed with diaminobenzidine (Sigma).

Results

Mutant-specific alteration of SOD1 solubility in fALS-linked H46R SOD1 transgenic mice

In this study, we used fALS-linked H46R SOD1 transgenic mice as reported previously [28]. To examine the fALS-linked mutation-dependent change of SOD1 solubility, we sequentially extracted spinal cords of mutant transgenic mice with severe motor impairment (~24 weeks of age) with PBS, 1% TX, 5% SDS, 8 M urea, and 88% FA (Fig. 1A), and then separated extracts by SDS–PAGE under the denaturing condition. In 24-week-old non-transgenic littermates and 38-week-old wild-type SOD1

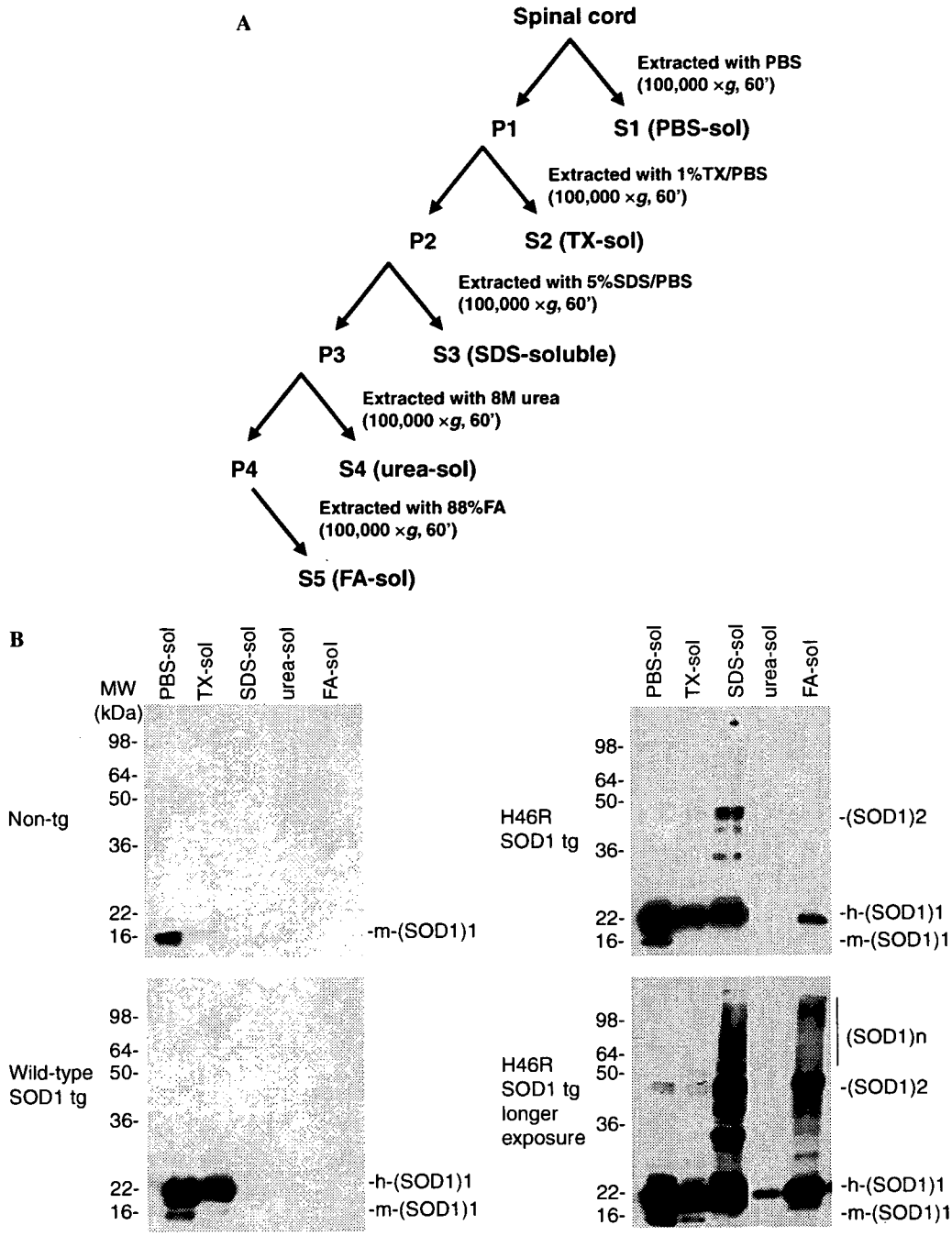

Fig. 1. Mutant-specific alteration of SOD1 solubility in spinal cords from fALS-linked H46R SOD1 transgenic mice. (A) Schematic representation of the sequential extraction steps. (B) Western blot analysis of spinal cords from 24-week-old non-transgenic mice (Non-tg) (upper left panel), 38-week-old wild-type SOD1 transgenic mice (Wild-type SOD1 tg) (lower left panel), and mutant H46R SOD1 transgenic mice at end stage (H46R SOD1 tg) (upper right panel). Ten micrograms of protein from each of the PBS-soluble fraction (PBS-sol), the TX-soluble fraction (TX-sol), the SDS-soluble fraction (SDS-sol), and the urea-soluble fraction (urea-sol) and equal aliquots of the FA-soluble fraction (FA-sol) were subjected to 15% polyacrylamide gels under reducing conditions. Western blots were probed with SOD1-100 antibody, which recognizes both human SOD1 (h-SOD1) and mouse endogenous SOD1 (m-SOD1). The lower right panel (identical to the upper right panel) was exposed to the film for a longer time.

transgenic mice, endogenous mouse SOD1, and wild-type human SOD1 were detected as monomers migrating at 16-kDa and 22-kDa, respectively, in the PBS- and 1% TX-soluble fractions (Fig. 1B). This finding may be explained by the fact that normal SOD1 is a soluble protein located predominantly in the cytosol and less within the membranous organelle such as mitochondrial intermembrane space [4]. In contrast to the control mouse SDS-soluble fraction that was virtually devoid of SOD1, intense bands of SOD1 were found in the SDS-soluble fraction of mutant transgenic mice (Fig. 1B). In the fraction, the anti-SOD1 antibody (SOD1-100) recognized 22-kDa bands ((SOD1)1; it represents SOD1 monomer), ~44-kDa bands ((SOD1)2; apparent molecular weight of (SOD1)2 shows 2-fold to 22-kDa monomer, being consistent with SOD1 dimer as previously reported [19]), and multiple bands above 44-kDa ((SOD1)n; it represents high-molecular-weight (HMW) species). Also, ~28 and ~36-kDa bands were observed in the SDS-soluble fraction. These bands may represent proteolytic fragments from HMW species, but the exact origin was unknown in this study. SOD1 monomers, dimers, and HMW species were further recovered in the FA-soluble fraction, whereas a small amount of monomeric SOD1, but not HMW species, was detected in the urea-soluble fraction, indicating that FA-soluble SOD1 species were not simply carried over from the prior urea extracts (Fig. 1B). TX-insoluble/SDS-soluble (designated as SDS-soluble) species are characterized by an alteration of solubility to distinguish mutant H46R SOD1 from a wild-type one. Also, mutant H46R SOD1 contained SDS-stable oligomers with diverse solubility in detergents or denaturants.

Age-dependent alteration of SOD1 solubility in H46R SOD1 transgenic mice

As described in our previous report, the H46R SOD1 transgenic mice showed motor dysfunction with aging, and the stages of motor dysfunction could be classified into four time periods based on the Rotarod test: 13 weeks, 17 weeks, 21 weeks, and later 23 weeks of age were designated as the early presymptomatic stage (EP), late presymptomatic stage (LP), symptomatic stage (SS), and end stage (ES), respectively [28]. To clarify the alteration of SOD1 solubility with aging in mutant SOD1 transgenic mice, we compared the levels of SOD1 species, which were biochemically fractionated as described above, in the different stages (Figs. 2A and B). The levels of both PBS-soluble and TX-soluble SOD1 monomers showed no statistically significant difference between stages, although they had a tendency to decrease with aging (Figs. 2A and B). In the SDS-soluble fraction, mutant SOD1 monomers and dimers were clearly detected at EP. The ratios of SOD1 monomers at EP and LP versus ES were $20.52 \pm 6.41\%$ (mean $\pm$ SD) and $45.88 \pm 2.30\%$, respectively. In addition, the ratios of SOD1 dimers at EP and LP versus ES were $29.38 \pm 21.20\%$ and $68.47 \pm 10.27\%$, respectively. On the other hand, the levels of SOD1 HMW species showed the later elevation at the period between LP and SS. These findings indicate that the increase of SDS-dissociable soluble SOD1 monomers and SDS-stable soluble SOD1 dimers occurred between EP and LP before onset ($n = 3$, $p = 0.017$ and $p = 0.005$, respectively) (Fig. 2B). In the FA-soluble fraction, a small number of SOD1 monomers were also seen at EP, but there was no significant difference in the levels of monomers between EP and LP. The ratios of SOD1 monomers at LP and SS versus ES were $32.31 \pm 12.99\%$ and $68.30 \pm 17.03\%$, respectively. The ratios of SOD1 dimers at LP and SS versus ES were $12.73 \pm 6.27\%$ and $41.42 \pm 4.50\%$, respectively. The levels of FA-soluble SOD1 monomers and FA-soluble dimers significantly increased between LP and SS ($p = 0.036$ and $p < 0.001$, respectively), while the levels of FA-soluble SOD1 HMW species elevated later in the period between SS and ES (Figs. 2A and B). The levels of SDS-dissociable soluble monomers and SDS-stable soluble dimers elevated earlier than the SDS-stable soluble HMW species and FA-soluble species.

To examine the relation between the alteration of SOD1 solubility and the formation of SOD1-inclusions with aging, we immunostained mouse spinal cords in four different stages with monoclonal anti-SOD1 antibody (Fig. 2C). At EP, we did not detect any kind of SOD1-inclusions. SOD1-inclusions in the neuropil appeared at SS, and the number of SOD1-inclusions increased between SS and ES (Fig. 2C). SOD1-inclusions increased after disease onset, indicating that the accumulation of SDS-dissociable soluble SOD1 monomers and SDS-stable soluble dimers precedes the appearance of SOD1-inclusions.

The increase of Hsp70/40 in the SDS-soluble fraction with aging in H46R SOD1 transgenic mice

To examine how the mutant-specific alteration of SDS solubility is associated with the molecular chaperone system, the fractionated samples prepared above were analyzed by Western blotting using antibodies to Hsp70 and Hsp40. Hsp70 and Hsp40 were found to be rich in the PBS-soluble and the TX-soluble fractions (Fig. 3A). PBS- and TX-soluble Hsp70 and Hsp40 showed constant levels in all stages of mutant transgenic mice and were not different from those in 24-week-old non-transgenic littermates and 38-week-old wild-type SOD1 transgenic mice (Fig. 3A). In the SDS-soluble fraction, the levels of Hsp70 and Hsp40 in mutant transgenic mice at LP were higher than those in the control mice at later 24 weeks of age. The levels of Hsp70 and Hsp40 in the SDS-soluble fractions elevated at the period between EP and LP in mutant transgenic mice (Fig. 3A). To clarify how the increase of Hsp70 and Hsp40 in the SDS-soluble fraction reflects in histopathological change with aging, we immunostained the lumbar spinal cords with antibodies to Hsp70 and Hsp40 (Fig. 3B). SOD1-positive inclusions were intensely stained with the antibody to Hsp70 as previously reported and faintly reacted with the antibody to Hsp40 in

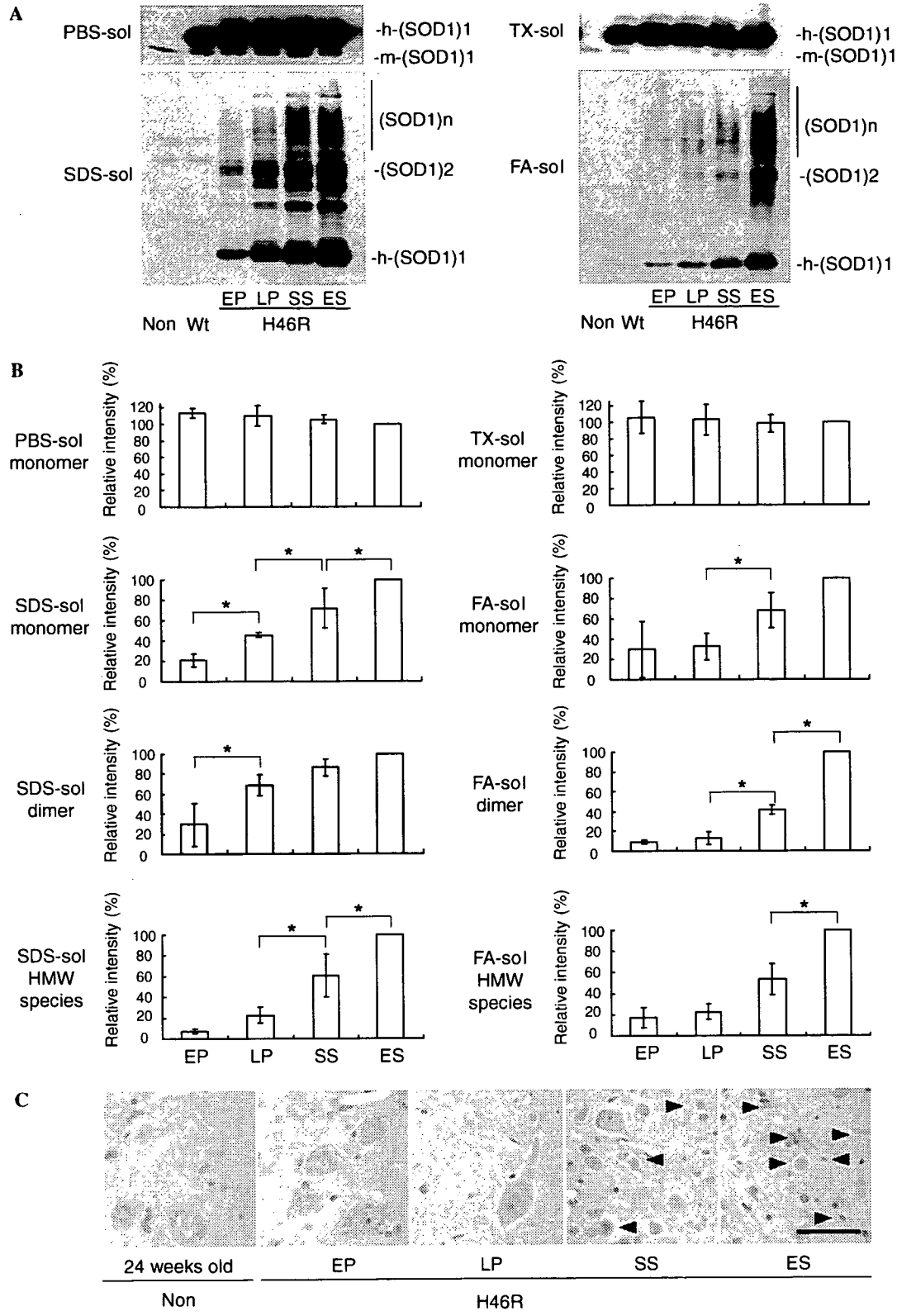

Fig. 2. Age-dependent alteration of SOD1 in spinal cords from H46R SOD1 transgenic mice. (A) The spinal cords of 24-week-old non-transgenic littermates (Non), 38-week-old wild-type SOD1 transgenic mice (Wt), and H46R SOD1 transgenic mice (H46R) at early presymptomatic stage (EP), late presymptomatic stage (LP), symptomatic stage (SS), and end stage (ES) were sequentially fractionated. Ten micrograms of protein from each of the PBS-soluble fraction (PBS-sol), the TX-soluble fraction (TX-sol), and the SDS-soluble fraction (SDS-sol), and equal aliquots of the FA-soluble fraction (FA-sol) were loaded on the gel and then immunoblotted with SOD1-100 antibody. (B) The graphs represent relative intensities of H46R SOD1 species at each stage ($n = 3$, bars represent mean ± SD,*$P < 0.05$). (C) Immunohistochemical analysis of lumbar spinal cords (L_{4-5}) of 24-week-old non-transgenic littermates (Non) and H46R SOD1 transgenic mice (H46R) at four stages. These sections were immunostained with monoclonal anti-SOD1 antibody specific to human SOD1. Scale bars = 50 μm. Arrowheads indicate SOD1-immunoreactive structures.

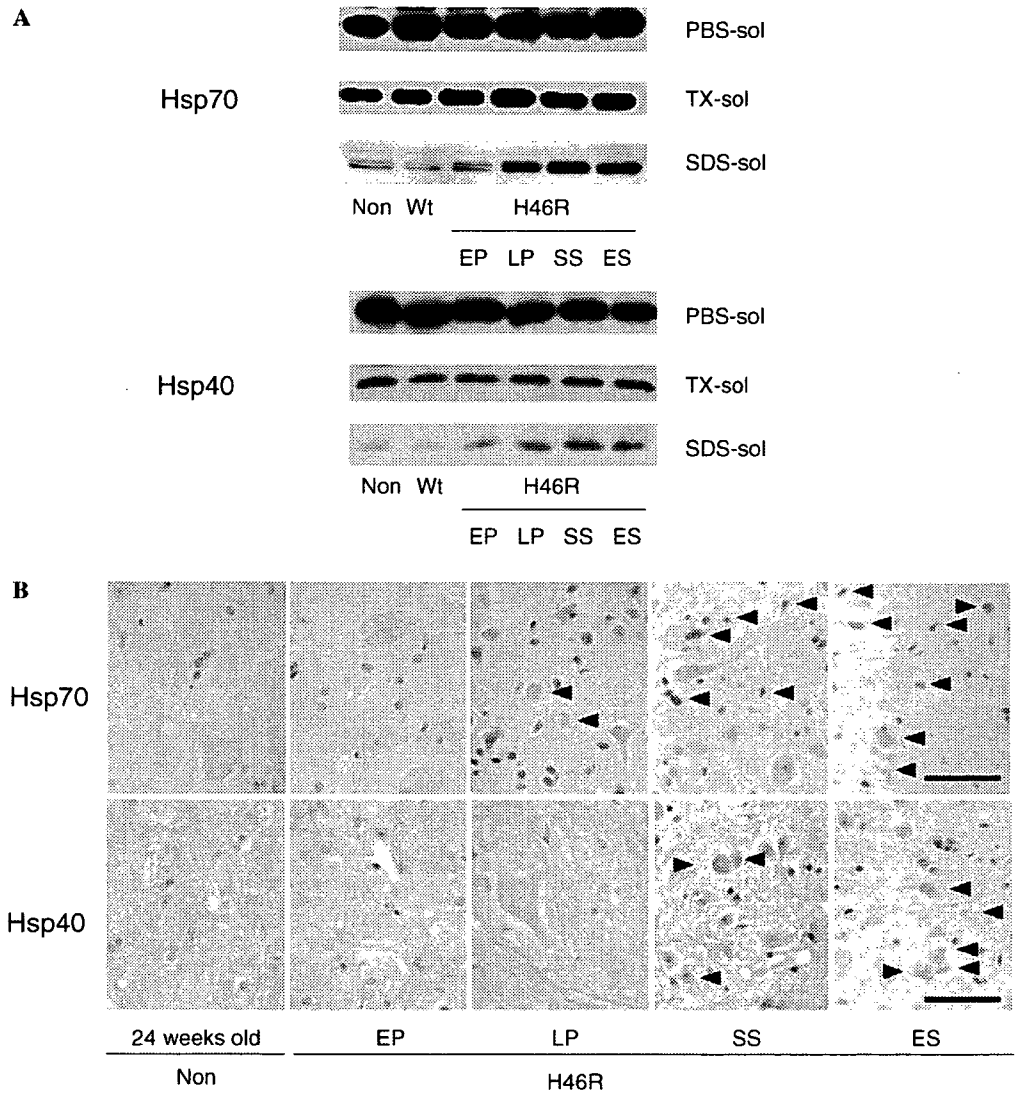

Fig. 3. (A) Increase of Hsp70 and Hsp40 in the SDS-soluble fraction from H46R SOD1 transgenic mice. The fractionated samples used in Fig. 2 were analyzed by Western blotting using anti-Hsp70 and anti-Hsp40 antibodies. Ten micrograms of total protein from each fraction was loaded on each lane. (B) Time course analysis of Hsp-immunoreactive structures. These sections were immunostained with anti-Hsp70 antibody and anti-Hsp40 antibody. Scale bars = 50 μm. Arrowheads indicate immunoreactive structures of each antibody.

the serial sections (data not shown). Although a small number of Hsp70-positive structures were found in neuropil at LP, the increase of SOD1-inclusions containing Hsp70 immunoreactivities was remarkable after SS (Fig. 3B). Similarly, Hsp40-positive structures increased from SS (Fig. 3B). The present data showed that the increase of Hsp70 and Hsp40 in the SDS-soluble fraction appeared along with the increase of SDS-dissociable soluble SOD1 monomers and SDS-stable soluble dimers. This increase of Hsp70 and Hsp40 occurred before the accumulation of visible inclusions with Hsp70 and Hsp40 immunoreactivities.

Inhibition of the proteasome activity promotes the change of SOD1 solubility in cells expressing H46R SOD1

The fALS-linked mutant misfolded SOD1 protein is reported to be degraded by the proteasome pathway [16,17,19,20]. To see how inhibition of the proteasome pathway influences mutant SOD1 solubility, we examined COS-7 cells transiently overexpressing either wild-type SOD1-FLAG or H46R SOD1-FLAG in the presence or absence of proteasome inhibitor MG132. In this experiment, FLAG-tagged SOD1 was used for discriminating exogenous SOD1 from endogenous SOD1 by migrating more slowly. Collected cell pellets were sequentially extracted with PBS, 1% TX, and 5% SDS. In the PBS-soluble and the TX-soluble fractions, the levels of mutant SOD1 as well as wild-type SOD1 slightly increased when MG132 was added in a dose-dependent manner (Fig. 4A). In the SDS-soluble fraction, a small amount of wild-type monomeric SOD1 was seen in the absence of MG132. The levels of wild-type SOD1 monomers increased without generating HMW species in the presence of 10 μM MG132. On the other hand, in the SDS-soluble fraction, mutant SOD1 monomers and dimers were obviously

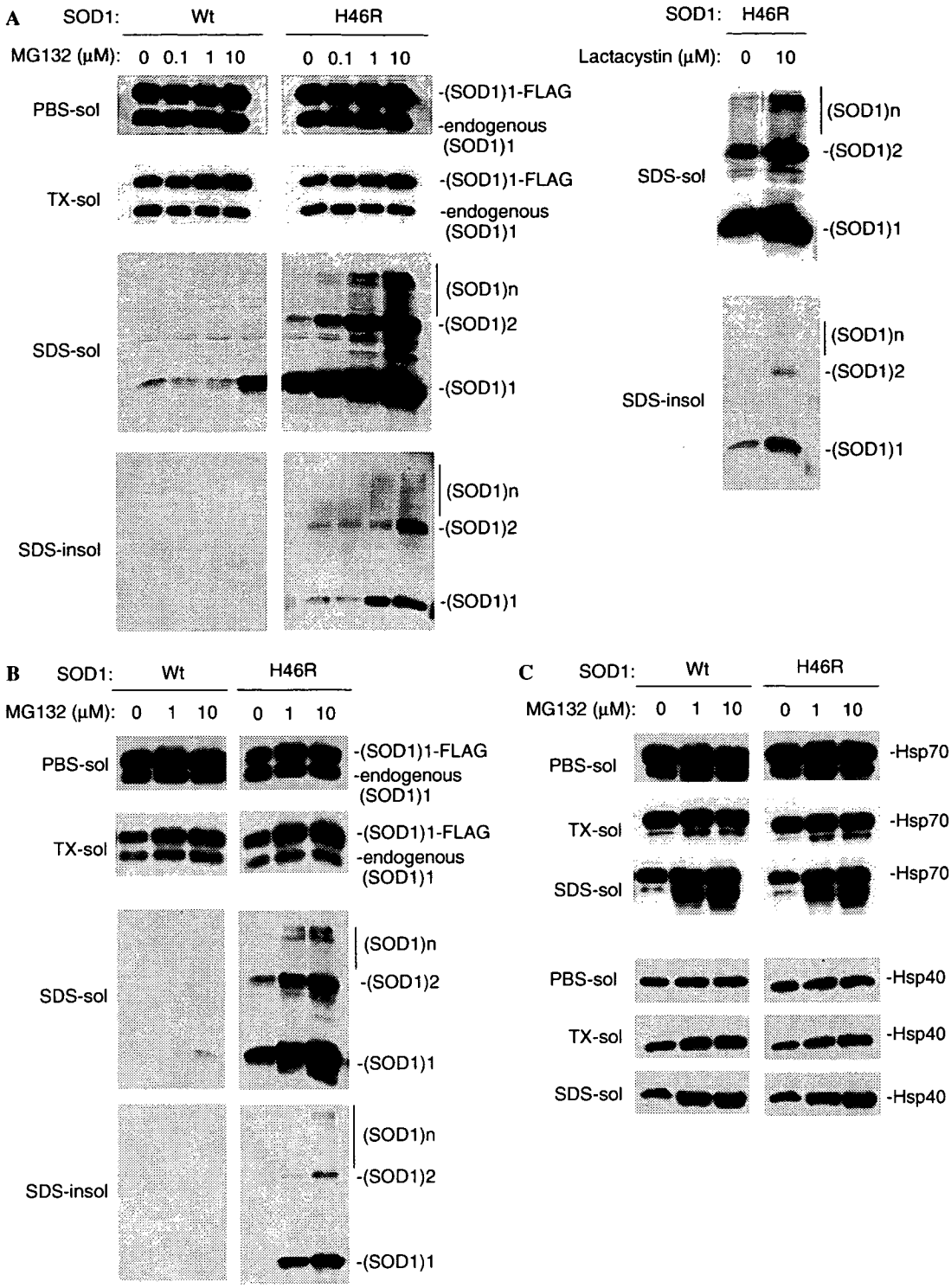

Fig. 4. Alteration of H46R SOD1 solubility in COS-7 and SH-SY5Y cells by treatment with proteasome inhibitors. COS-7 cells (A) and SH-SY5Y cells (B,C) were transiently transfected with either wild-type SOD1-FLAG pcDNA3.1 or H46R SOD1-FLAG pcDNA3.1. At 24 h after transfection, the culture medium was replaced with a fresh one containing the indicated concentrations of proteasome inhibitor, either MG132 (left panels of (A) and all panels of (B)) or lactacystin (right panels of (A)). Cells were incubated for an additional 24 h. Collected cell pellets were serially fractionated to the PBS-soluble fraction (PBS-sol), the TX-soluble fraction (TX-sol), the SDS-soluble fraction (SDS-sol), and the SDS-insoluble fraction (SDS-insol). Ten micrograms of protein from each of the PBS-soluble fraction, the TX-soluble fraction, and the SDS-soluble fraction, and equal aliquots of the SDS-insoluble fraction were subjected to the gel and immunoblotted with SOD1-100 (A,B). (C) The levels of both endogenous Hsp70 and Hsp40 were elevated in the SDS-soluble fraction from cells expressing wild-type SOD1 as well as mutant SOD1 in an MG-132 dose-dependent manner. The fractionated samples used in (B) were analyzed by Western blotting using anti-Hsp70 and anti-Hsp40 antibodies.

detected in the absence of MG132 and showed a significant increase in generating HMW species by treatment with MG132 in a dose-dependent manner (Fig. 4A). Similarly, in the SDS-insoluble fraction, the levels of mutant SOD1 monomers, dimers, and HMW species elevated by treatment with MG132 in a dose-dependent manner, while wild-type SOD1 was not detected (Fig. 4A). Dose-dependent treatment with MG132 further showed that the elevation of SDS-dissociable soluble mutant SOD1 monomers and SDS-stable soluble dimers preceded that of SDS-stable soluble HMW species and SDS-insoluble species. Treatment with another specific proteasome inhibitor, lactacystin, also caused the accumulation of SDS-soluble and SDS-insoluble mutant SOD1 species in COS-7 cells, although to a lesser extent (Fig. 4A). We further confirmed the effect of MG132 on the alteration of SOD1 solubility in human neuroblastoma SH-SY5Y cells. By treatment with MG132, SDS-soluble and SDS-insoluble mutant SOD1 monomers, dimers, and HMW species accumulated in mutant-specific and dose-dependent manners in SH-SY5Y cells similar to COS-7 cells (Fig. 4B). The elevation of SDS-dissociable soluble mutant SOD1 monomers and SDS-stable soluble dimers also preceded that of SDS-stable soluble HMW species and SDS-insoluble species. In SH-SY5Y cells expressing mutant SOD1, the levels of both endogenous Hsp70 and Hsp40 were elevated in the SDS-soluble fraction in an MG-132 dose-dependent manner (Fig. 4C). However, the increase of endogenous Hsp70 and Hsp40 levels in the SDS-soluble fraction was similarly observed in cells expressing wild-type SOD1 (Fig. 4C). These results showed that inhibition of the proteasome activity in mutant SOD1 expressed cells recapitulated the alteration of SOD1 solubility with aging in mutant transgenic mice. Inhibition of the proteasome activity initially led to the accumulation of SDS-dissociable soluble mutant SOD1 monomers and SDS-stable soluble dimers prior to that of SDS-stable soluble HMW species and SDS-insoluble species irrespective of the increase of endogenous Hsp70 and Hsp40.

Effect of overexpression of Hsp70 on the accumulation of SDS-soluble and SDS-insoluble mutant SOD1 species

Overexpression of Hsp70 has been reported to reduce the SOD1-aggregate formation and prolong cellular viability in a cellular model of fALS [23]. As described in our previous report [20], overexpression of mutant SOD1 pEF-BOS in COS-7 cells causes higher expression levels of SOD1 than overexpression of mutant SOD1 pcDNA3.1, and a large amount of SDS-insoluble mutant SOD1 appears without adding proteasome inhibitor. By taking advantage of this high-expression system, we investigated cells co-transfected with mutant H46R SOD1 cDNA and a 4-fold molar excess of Hsp cDNA to see the effect of Hsp70 and Hsp40 on the levels of altered insoluble SOD1 species (Fig. 5A). Overexpression of Hsp70 obviously reduced the levels of SDS-dissociable soluble mutant SOD1 monomers, SDS-stable soluble dimers, and SDS-stable soluble HMW species, compared to co-expression of the empty vector (Fig. 5A). Overexpression of Hsp40 showed a weaker effect on the levels of SDS-soluble mutant SOD1 species (Fig. 5A). Co-overexpression with Hsp70 plus Hsp40 enhanced the effect of Hsp70 on a decrease of the levels of SDS-stable soluble mutant SOD1 dimers and HMW species (Fig. 5A). In the SDS-insoluble fraction, overexpression of Hsp70 also led to a reduction in the levels of SDS-dissociable insoluble mutant SOD1 monomers, SDS-stable insoluble dimers, and SDS-stable insoluble HMW species, and the effect was enhanced by co-overexpression of Hsp40 (Fig. 5A). This finding was also observed in cells expressing different fALS-linked mutant G93A SOD1 (data not shown). To further examine the molecular mechanism by which overexpression of Hsp70 reduced insoluble mutant SOD1 species, cells were co-transfected with H46R SOD1 and Hsp70 cDNAs in various molar ratios (Fig. 5B). The levels of mutant SOD1 monomers, dimers, and HMW species in the SDS-soluble fraction as well as in the SDS-insoluble fraction decreased in negative correlation to the amounts of transfected Hsp70 cDNA (Figs. 5B and C). On the other hand, the levels of mutant SOD1 monomers in the PBS-soluble and TX-soluble fractions did not increase, in sharp contrast to the significant reduction of the amount of SDS-soluble species by overexpression of Hsp70 (Figs. 5B and C). These findings demonstrated that overexpressed Hsp70 modulated the levels at SDS-dissociable soluble mutant SOD1 monomers and SDS-stable soluble dimers as misfolded proteins and preferentially forwarded abnormally insoluble SOD1 species to degradation rather than to refolding.

Discussion

Although wild-type SOD1 is principally a soluble, cytosolic protein [4], fALS-linked mutant SOD1 has a tendency to assemble as insoluble aggregates, which are immunohistochemically observed as cytoplasmic inclusions in patients with fALS having SOD1 mutation [10]. There has been controversy about whether such inclusions are a cause or simply a result of the neuronal degeneration. Immunohistochemical experiments do not rule out the possibility that mutant SOD1 aggregates can damage motor neurons, even though microscopically visible inclusions are absent in the early period. In agreement with the previous finding [16,19], our immunohistochemical data demonstrated that SOD1-positive inclusions appeared after disease onset, and the accumulation of SOD1-positive inclusions was parallel to the elevation of most insoluble SOD1 species recovered in the FA-soluble fraction. On the other hand, we revealed that mutant H46R SOD1 began to significantly alter its solubility to SDS-dissociable soluble monomers and SDS-stable soluble dimers earlier than the appearance of visible SOD1-positive inclusions. These findings suggest that complexes of SDS-dissociable soluble SOD1 monomers and SDS-stable soluble dimers were much smaller in

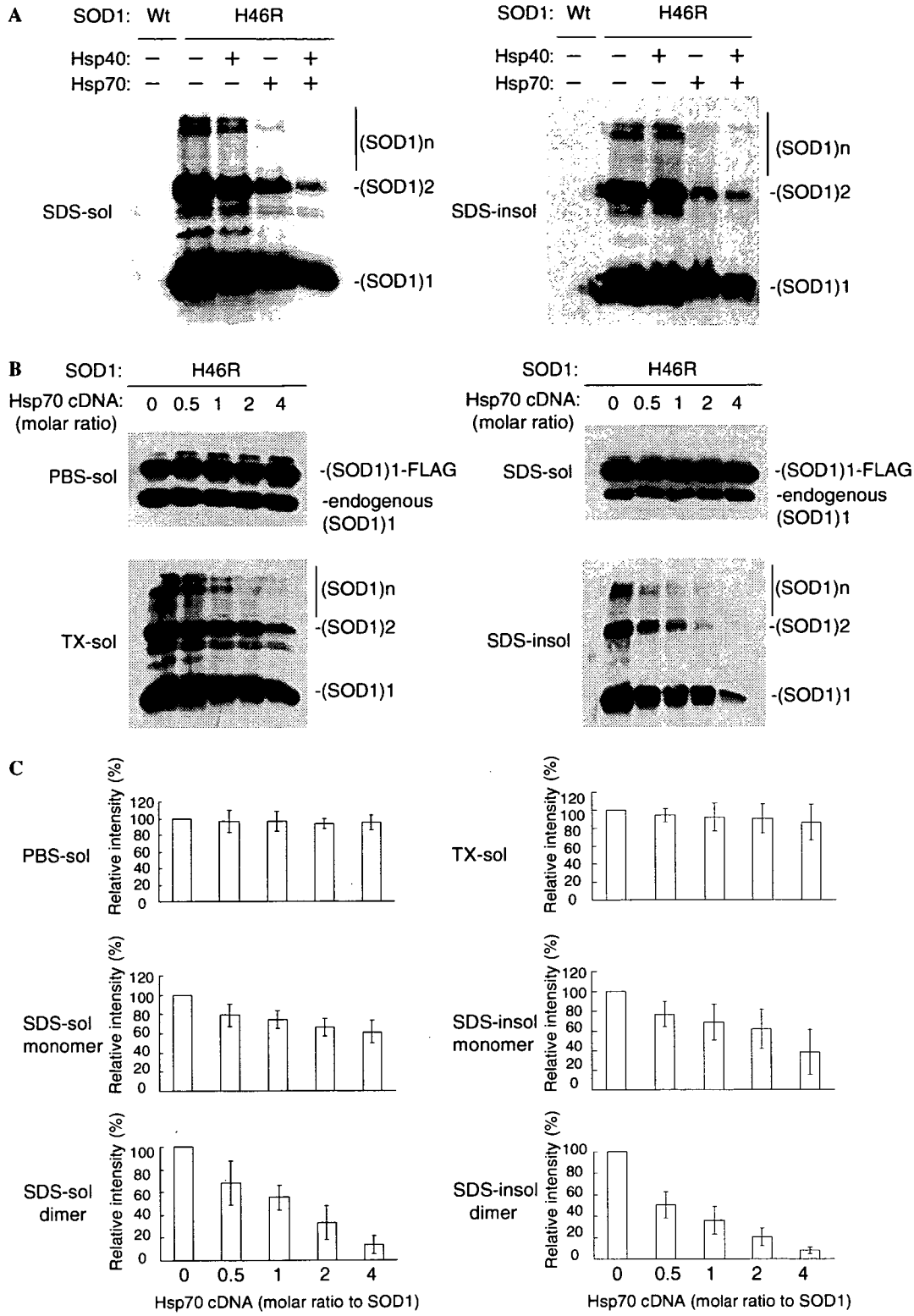

Fig. 5. The effect of overexpression of Hsp70 and Hsp40 on the level of altered insoluble mutant SOD1 in intact cells. (A) Western blots of COS-7 cells co-transfected with H46R SOD1-FLAG pEF-BOS and either pCMV-Hsp70 or pRC-Hsp40 (molar ratio of Hsp versus SOD1 cDNA was 4:1) using SOD1-100 antibody. Proteins from the SDS-soluble (SDS-sol) and SDS-insoluble (SDS-insol) fractions were loaded to the gel and immunoblotted with SOD1-100 antibody. (B) Western blot analysis of cells co-transfected with H46R SOD1-FLAG pEF-BOS and various amounts of Hsp70 cDNA. Molar ratios of pCMV-Hsp70 versus H46R SOD1-FLAG pEF-BOS are indicated in the figure. Forty-eight hours after transfection, cells were harvested and fractionated. Proteins from each fraction were analyzed by Western blotting using an SOD1-100 antibody. (C) The graphs show the relative intensities of H46R SOD1 monomers and dimers in each fraction shown in (B). The relative intensities were quantified by densitometry and normalized to bands from cells transfected with the empty vector ($n = 3$, bars represent mean ± SD).

size than visible inclusions, and the presence of visible inclusions composed of highly insoluble aggregates contributes less to the early pathological event.

Our findings are relevant to the previous reports that detergent-insoluble dimers and HMW species were found before onset of motor disability and the appearance of pathological SOD1-aggregates in mutant SOD1 transgenic mice [16,19]. However, in these preceding experiments, the alteration of mutant SOD1 solubility was assessed by fractionation using only one detergent. By the sequential extraction of mutant transgenic mouse spinal cords with PBS and TX containing buffer for removing cytosolic and mitochondrial SOD1 with normal solubility equivalent to wild-type SOD1, we separated H46R SOD1 into three different kinds of mutant-specific insoluble species, indicating that insoluble mutant SOD1 did not consist of a uniform species. To see whether SDS-dissociable soluble monomers, in addition to SDS-stable soluble dimers, represented early misfolded intermediates, we have investigated the alteration of SOD1 solubility using a cell culture model of fALS. Treatment with proteasome inhibitors caused the accumulation of SDS-dissociable soluble mutant H46R SOD1 monomers and SDS-stable soluble dimers earlier than that of SDS-stable soluble HMW species and SDS-insoluble species. This finding resembled the age-dependent alteration of SOD1 solubility in mutant H46R SOD1 transgenic mice. In contrast, overexpression of Hsp70 reduced the levels of SDS-dissociable soluble mutant H46R SOD1 monomers and SDS-stable soluble dimers. These findings indicate that SDS-dissociable soluble mutant SOD1 monomers and SDS-stable soluble dimers are degraded by the proteasome pathway and are modulated by molecular chaperones as misfolded intermediates. The previous in vitro study showed that a normal homodimer of SOD1 dissociates to an aggregation-prone monomeric intermediate by oxidation [32]. Further experiments would be necessary to see how potentially aggregation-promoting modifications, such as oxidation and nitration, relate to the alteration of SOD1 solubility.

Several reports showed that Hsp70 and its co-chaperone Hsp40 were involved in the aggregation process or the degradation of SOD1 [11,33], and Hsp70 and Hsp40 suppress SOD1 aggregate formation and improve neurite outgrowth [34]. Although in the previous report up-regulation of Hsp70 was not observed in the spinal cords of mutant SOD1 transgenic mice in contrast to cultured cells overexpressing mutant SOD1 [23], we found that the levels of Hsp70 and Hsp40 in mutant SOD1 transgenic mice increased in the SDS-soluble fraction before disease onset. This observation is consistent with the report that Hsp70 interacts with detergent-insoluble SOD1 rather than detergent-soluble SOD1 in cells [33]. However, it should be noted that endogenous Hsp70 and Hsp40 in the SDS-soluble fraction do not suppress accumulation of insoluble mutant SOD1 in the present H46R SOD1 transgenic mice. Furthermore, Liu et al. [35] showed that elevation of Hsp70 does not affect ALS disease onset and survival in several types of mutant SOD1 transgenic mice co-overexpressing Hsp70 at ~10-fold higher levels than control mice, suggesting that there was no benefit from chronically elevated Hsp70. In cells, overexpression of Hsp70 reduced the levels of SDS-soluble and SDS-insoluble mutant H46R SOD1, whereas it did not lead to the elevation of PBS-soluble and TX-soluble SOD1 levels. This result implies that overexpression of Hsp70 had an effect on the levels of mutant-specific insoluble SOD1 species by forwarding them to the degradation pathway rather than refolding them to a normal soluble pool of SOD1. Adachi et al. [36] reported that overexpression of Hsp70 decreased soluble monomeric androgen receptor (AR) protein in addition to HMW mutant AR protein in double transgenic mice expressing mutant AR protein and Hsp70, suggesting that Hsp70 enhanced mutant AR degradation. Since inhibition of the proteasome activity in cells had a strong effect on the accumulation of insoluble mutant SOD1 with up-regulation of endogenous Hsp70 and Hsp40, the discrepancy in beneficial effects of Hsp70 between cellular and mouse models of fALS may be explained by several possibilities. First, the diminishing of the proteasome activity may generate abundant misfolded proteins whose concentration exceeds the capacity of up-regulated endogenous Hsp70/40. Second, the main function of Hsp70 is to facilitate the proteasome pathway-dependent clearance of misfolded SOD1. Third, the accumulation of insoluble SOD1 species directly impairs the chaperone function of Hsp70 [37]. An approach for examining the toxicity of SDS-dissociable soluble mutant SOD1 monomers and SDS-stable soluble dimers may provide a clue to prevent a further accumulation of potentially toxic misfolded protein complexes in fALS.

Acknowledgments

This work was supported by Research Grants from the Japan ALS association (S.A.), a Grant-in-Aid for Scientific Research on Priority Areas (Advanced Brain Science Project) from the Ministry of Education, Culture, Sports, Science and Technology, Japan (S.A.), and a Research Grant on Measures for Intractable Diseases from the Ministry of Health, Labour and Welfare (T.K.).

References

[1] D.R. Rosen, T. Siddique, D. Patterson, D.A. Figlewicz, P. Sapp, A. Hentati, D. Donaldson, J. Goto, J.P. O'Regan, H.X. Deng, et al., Mutations in Cu/Zn superoxide dismutase gene are associated with familial amyotrophic lateral sclerosis, Nature 362 (1993) 59–62.

[2] M.E. Cudkowicz, D. McKenna-Yasek, P.E. Sapp, W. Chin, B. Geller, D.L. Hayden, D.A. Schoenfeld, B.A. Hosler, H.R. Horvitz, R.H. Brown, Epidemiology of mutations in superoxide dismutase in amyotrophic lateral sclerosis, Ann. Neurol. 41 (1997) 210–221.

[3] J.S. Valentine, P.J. Hart, Misfolded CuZnSOD and amyotrophic lateral sclerosis, Proc. Natl. Acad. Sci. USA 100 (2003) 3617–3622.

[4] A. Okado-Matsumoto, I. Fridovich, Subcellular distribution of superoxide dismutases (SOD) in rat liver: Cu,Zn-SOD in mitochondria, J. Biol. Chem. 276 (2001) 38388–38393.

[5] A.G. Reaume, J.L. Elliott, E.K. Hoffman, N.W. Kowall, R.J. Ferrante, D.F. Siwek, H.M. Wilcox, D.G. Flood, M.F. Beal, R.H. Brown Jr., R.W. Scott, W.D. Snider, Motor neurons in Cu/Zn superoxide dismutase-deficient mice develop normally but exhibit enhanced cell death after axonal injury, Nat. Genet. 13 (1996) 43–47.

[6] M.E. Gurney, H. Pu, A.Y. Chiu, M.C. Dal Canto, C.Y. Polchow, D.D. Alexander, J. Caliendo, A. Hentati, Y.W. Kwon, H.X. Deng, et al., Motor neuron degeneration in mice that express a human Cu,Zn superoxide dismutase mutation, Science 264 (1994) 1772–1775.

[7] M.E. Ripps, G.W. Huntley, P.R. Hof, J.H. Morrison, J.W. Gordon, Transgenic mice expressing an altered murine superoxide dismutase gene provide an animal model of amyotrophic lateral sclerosis, Proc. Natl. Acad. Sci. USA 92 (1995) 689–693.

[8] P.C. Wong, C.A. Pardo, D.R. Borchelt, M.K. Lee, N.G. Copeland, N.A. Jenkins, S.S. Sisodia, D.W. Cleveland, D.L. Price, An adverse property of a familial ALS-linked SOD1 mutation causes motor neuron disease characterized by vacuolar degeneration of mitochondria, Neuron 14 (1995) 1105–1116.

[9] L.I. Bruijn, M.W. Becher, M.K. Lee, K.L. Anderson, N.A. Jenkins, N.G. Copeland, S.S. Sisodia, J.D. Rothstein, D.R. Borchelt, D.L. Price, D.W. Cleveland, ALS-linked SOD1 mutant G85R mediates damage to astrocytes and promotes rapidly progressive disease with SOD1-containing inclusions, Neuron 18 (1997) 327–338.

[10] N. Shibata, A. Hirano, M. Kobayashi, T. Siddique, H.X. Deng, W.Y. Hung, T. Kato, K. Asayama, Intense superoxide dismutase-1 immunoreactivity in intracytoplasmic hyaline inclusions of familial amyotrophic lateral sclerosis with posterior column involvement, J. Neuropathol. Exp. Neurol. 55 (1996) 481–490.

[11] M. Watanabe, M. Dykes-Hoberg, V.C. Culotta, D.L. Price, P.C. Wong, J.D. Rothstein, Histological evidence of protein aggregation in mutant SOD1 transgenic mice and in amyotrophic lateral sclerosis neural tissues, Neurobiol. Dis. 8 (2001) 933–941.

[12] P.A. Jonsson, K. Ernhill, P.M. Andersen, D. Bergemalm, T. Brannstrom, O. Gredal, P. Nilsson, S.L. Marklund, Minute quantities of misfolded mutant superoxide dismutase-1 cause amyotrophic lateral sclerosis, Brain 127 (2004) 73–88.

[13] H.D. Durham, J. Roy, L. Dong, D.A. Figlewicz, Aggregation of mutant Cu/Zn superoxide dismutase proteins in a culture model of ALS, J. Neuropathol. Exp. Neurol. 56 (1997) 523–530.

[14] T. Koide, S. Igarashi, K. Kikugawa, R. Nakano, T. Inuzuka, M. Yamada, H. Takahashi, S. Tsuji, Formation of granular cytoplasmic aggregates in COS7 cells expressing mutant Cu/Zn superoxide dismutase associated with familial amyotrophic lateral sclerosis, Neurosci. Lett. 257 (1998) 29–32.

[15] M. Nagai, M. Aoki, I. Miyoshi, M. Kato, P. Pasinelli, N. Kasai, R.H. Brown Jr., Y. Itoyama, Rats expressing human cytosolic copper-zinc superoxide dismutase transgenes with amyotrophic lateral sclerosis: associated mutations develop motor neuron disease, J. Neurosci. 21 (2001) 9246–9254.

[16] J.A. Johnston, M.J. Dalton, M.E. Gurney, R.R. Kopito, Formation of high molecular weight complexes of mutant Cu, Zn-superoxide dismutase in a mouse model for familial amyotrophic lateral sclerosis, Proc. Natl. Acad. Sci. USA 97 (2000) 12571–12576.

[17] K. Puttaparthi, C. Wojcik, B. Rajendran, G.N. DeMartino, J.L. Elliott, Aggregate formation in the spinal cord of mutant SOD1 transgenic mice is reversible and mediated by proteasomes, J. Neurochem. 87 (2003) 851–860.

[18] J. Wang, G. Xu, D.R. Borchelt, High molecular weight complexes of mutant superoxide dismutase 1: age-dependent and tissue-specific accumulation, Neurobiol. Dis. 9 (2002) 139–148.

[19] M. Urushitani, J. Kurisu, K. Tsukita, R. Takahashi, Proteasomal inhibition by misfolded mutant superoxide dismutase 1 induces selective motor neuron death in familial amyotrophic lateral sclerosis, J. Neurochem. 83 (2002) 1030–1042.

[20] S. Tobisawa, Y. Hozumi, S. Arawaka, S. Koyama, M. Wada, M. Nagai, M. Aoki, Y. Itoyama, K. Goto, T. Kato, Mutant SOD1 linked to familial amyotrophic lateral sclerosis, but not wild-type SOD1, induces ER stress in COS7 cells and transgenic mice, Biochem. Biophys. Res. Commun. 303 (2003) 496–503.

[21] D.H. Hyun, M. Lee, B. Halliwell, P. Jenner, Proteasomal inhibition causes the formation of protein aggregates containing a wide range of proteins, including nitrated proteins, J. Neurochem. 86 (2003) 363–373.

[22] E. Kabashi, J.N. Agar, D.M. Taylor, S. Minotti, H.D. Durham, Focal dysfunction of the proteasome: a pathogenic factor in a mouse model of amyotrophic lateral sclerosis, J. Neurochem. 89 (2004) 1325–1335.

[23] W. Bruening, J. Roy, B. Giasson, D.A. Figlewicz, W.E. Mushynski, H.D. Durham, Up-regulation of protein chaperones preserves viability of cells expressing toxic Cu/Zn-superoxide dismutase mutants associated with amyotrophic lateral sclerosis, J. Neurochem. 72 (1999) 693–699.

[24] C.A. Ross, M.A. Poirier, Protein aggregation and neurodegenerative disease, Nat. Med. 10 (Suppl.) (2004) S10–S17.

[25] A.A. Michels, B. Kanon, A.W. Konings, K. Ohtsuka, O. Bensaude, H.H. Kampinga, Hsp70 and Hsp40 chaperone activities in the cytoplasm and the nucleus of mammalian cells, J. Biol. Chem. 272 (1997) 33283–33289.

[26] Y. Kobayashi, A. Kume, M. Li, M. Doyu, M. Hata, K. Ohtsuka, G. Sobue, Chaperones Hsp70 and Hsp40 suppress aggregate formation and apoptosis in cultured neuronal cells expressing truncated androgen receptor protein with expanded polyglutamine tract, J. Biol. Chem. 275 (2000) 8772–8778.

[27] S. Arawaka, H. Hasegawa, A. Tandon, C. Janus, F. Chen, G. Yu, K. Kikuchi, S. Koyama, T. Kato, P.E. Fraser, P. St. George-Hyslop, The levels of mature glycosylated nicastrin are regulated and correlate with gamma-secretase processing of amyloid beta-precursor protein, J. Neurochem. 83 (2002) 1065–1071.

[28] R. Chang-Hong, M. Wada, S. Koyama, H. Kimura, S. Arawaka, T. Kawanami, K. Kurita, T. Kadoya, M. Aoki, Y. Itoyama, T. Kato, Neuroprotective effect of oxidized galectin-1 in a transgenic mouse model of amyotrophic lateral sclerosis, Exp. Neurol. 194 (2005) 203–211.

[29] C.J. Epstein, K.B. Avraham, M. Lovett, S. Smith, O. Elroy-Stein, G. Rotman, C. Bry, Y. Groner, Transgenic mice with increased Cu/Zn-superoxide dismutase activity: animal model of dosage effects in Down syndrome, Proc. Natl. Acad. Sci. USA 84 (1987) 8044–8048.

[30] H. Fujiwara, M. Hasegawa, N. Dohmae, A. Kawashima, E. Masliah, M.S. Goldberg, J. Shen, K. Takio, T. Iwatsubo, alpha-Synuclein is phosphorylated in synucleinopathy lesions, Nat. Cell. Biol. 4 (2002) 160–164.

[31] P.J. Kahle, M. Neumann, L. Ozmen, V. Muller, S. Odoy, N. Okamoto, H. Jacobsen, T. Iwatsubo, J.Q. Trojanowski, H. Takahashi, K. Wakabayashi, N. Bogdanovic, P. Riederer, H.A. Kretzschmar, C. Haass, Selective insolubility of alpha-synuclein in human Lewy body diseases is recapitulated in a transgenic mouse model, Am. J. Pathol. 159 (2001) 2215–2225.

[32] R. Rakhit, J.P. Crow, J.R. Lepock, L.H. Kondejewski, N.R. Cashman, A. Chakrabartty, Monomeric Cu,Zn-superoxide dismutase is a common misfolding intermediate in the oxidation models of sporadic and familial amyotrophic lateral sclerosis, J. Biol. Chem. 279 (2004) 15499–15504.

[33] G.A. Shinder, M.C. Lacourse, S. Minotti, H.D. Durham, Mutant Cu/Zn-superoxide dismutase proteins have altered solubility and interact with heat shock/stress proteins in models of amyotrophic lateral sclerosis, J. Biol. Chem. 276 (2001) 12791–12796.

[34] H. Takeuchi, Y. Kobayashi, T. Yoshihara, J. Niwa, M. Doyu, K. Ohtsuka, G. Sobue, Hsp70 and Hsp40 improve neurite outgrowth and suppress intracytoplasmic aggregate formation in cultured neuronal cells expressing mutant SOD1, Brain Res. 949 (2002) 11–22.

[35] J. Liu, L.A. Shinobu, C.M. Ward, D. Young, D.W. Cleveland, Elevation of the Hsp70 chaperone does not effect toxicity in mouse

models of familial amyotrophic lateral sclerosis, J. Neurochem. 93 (2005) 875–882.
[36] H. Adachi, M. Katsuno, M. Minamiyama, C. Sang, G. Pagoulatos, C. Angelidis, M. Kusakabe, A. Yoshiki, Y. Kobayashi, M. Doyu, G. Sobue, Heat shock protein 70 chaperone overexpression ameliorates phenotypes of the spinal and bulbar muscular atrophy transgenic mouse model by reducing nuclear-localized mutant androgen receptor protein, J. Neurosci. 23 (2003) 2203–2211.
[37] H. Tummala, C. Jung, A. Tiwari, C.M. Higgins, L.J. Hayward, Z. Xu, Inhibition of chaperone activity is a shared property of several Cu,Zn-superoxide dismutase mutants that cause amyotrophic lateral sclerosis, J. Biol. Chem. 280 (2005) 17725–17731.

Galectin-1 as a Potential Therapeutic Agent for Amyotrophic Lateral Sclerosis

T. Kato*, C.-H. Ren, M. Wada and T. Kawanami

Department of Neurology, Hematology, Metabolism, Endocrinology, and Diabetology (DNHMED), Yamagata University School of Medicine, 2-2-2 Iida-Nishi, Yamagata 990-9585, Japan

Abstract: Amyotrophic lateral sclerosis (ALS) is a fatal neurodegenerative disease that affects almost selectively motor neurons in the central nervous system. Most ALS patients die within five years of onset. One of the neuropathological features of ALS is an "axonal spheroid," a large swelling of a motor axon within the anterior horn of the spinal cord; this abnormal structure seems to be related to the pathogenesis of motor neuron degeneration in ALS. In 2001, using biochemical and immunohistochemical methods, we found an accumulation of galectin-1 in ALS spheroids. By immuno-electron microscopy, the galectin-1 accumulated in the spheroids was observed to be closely associated with neurofilaments. Furthermore, we observed a marked depletion of galectin-1 in the skin of ALS patients; another abnormality frequently observed in ALS. These findings, therefore, suggest that galectin-1 may be involved in the pathogenesis of ALS. It is known that an oxidized form of galectin-1 promotes axonal regeneration; however, it is not known whether oxidized galectin-1 has a beneficial or an adverse effect on the pathophysiology of ALS. To examine this issue, we administered oxidized galectin-1 to transgenic mice with H46R mutant SOD1, an ALS model mouse. The results showed that the administration of oxidized galectin-1 improved the motor activity, delayed the onset of symptoms, and prolonged the survival of the galectin-1-treated mice. Furthermore, the number of remaining motor neurons in the spinal cord was more preserved in the galectin-1-treated mice than in the non-treated mice. We conclude that galectin-1 could be a candidate agent for the treatment of ALS.

Key Words: Amyotrophic lateral sclerosis, ALS, galectin-1, motor neuron, spheroid, SOD1, skin, transgenic mouse.

1. INTRODUCTION

Amyotrophic lateral sclerosis (ALS) is one of the most serious neurological diseases, showing a relentless course to death [1]. Since its first description by Charcot in 1897, no curative treatment has been established in spite of a vast effort by neurologists and neuroscientists. However, from the early 1990s to the present, a series of discoveries concerning ALS has introduced numerous therapeutic investigations on ALS [2-4]. A remarkable discovery was the identification of mutated copper/zinc superoxide dismutase (SOD1) in some families with autosomal dominant ALS [5]. Subsequently, the establishment of SOD1 transgenic mice has facilitated the screening for potential drugs or compounds that could be beneficial for ALS [6]. Furthermore, the discovery of glutamate toxicity to motor neurons has led to the development of the first FDA-approved drug, riluzole, in 1995 [2], almost 100 years after Charcot's discovery of ALS.

At the present time, there are largely four lines of therapeutic approaches, based on neuroprotection, anti-oxidant, neurotrophic, and immunomodulation paradigms [7-16] (Table 1). Unexpectedly, although experiments using motor neuron culture systems or SOD1 transgenic mice have supported those paradigms, no clinical trial has shown truly successful results, with the exception of riluzole, which prolongs survival by about two months in ALS patients [17]. One explanation is that clinical trials with a single-drug therapy design probably could not significantly improve the symptoms of ALS. For this assumption, a combination therapy or cocktail therapy using several candidate agents for ALS has been carried out, and several studies have shown the additive effect on prolonging the life span [18]. Therefore, the search for new drugs or compounds for ALS is necessary to provide new combinations with known ones.

In this review, we present current information on galectin-1 that suggests that it is a candidate compound for clinical trials of ALS in the future. First, we give a brief description of the clinical and pathological features of ALS. Second, we report the results of our investigations that galectin-1 accumulates in the proximal portions of motor neuron axons in the ALS spinal cord [19], but decreases in the ALS skin [20]. The altered localization of galectin-1 in ALS patients has led us to experiments in which galectin-1 was administered to ALS model mice. Our study shows the beneficial effects of galectin-1 for the survival and motor function of ALS model mice, suggesting that galectin-1 may also be a potential therapeutic agent for human ALS. After reviewing recent clinical trials for ALS [2-4, 6], we would like to emphasize that galectin-1 could be a promising agent for ALS, especially when used in combination with other drugs for ALS.

2. CLINICAL FEATURES OF ALS

ALS is a neurodegenerative disease characterized by generalized motor weakness without sensory or cognitive

*Address correspondence to this author at the Chairman and Professor, Department of Neurology, Hematology, Metabolism, Endocrinology, and Diabetology (DNHMED), Yamagata University School of Medicine, 2-2-2 Iida-Nishi, Yamagata 990-9585, Japan; Tel: +81-23-628-5316; Fax: +81-23-628-5318; E-mail: tkato@med.id.yamagata-u.ac.jp

1389-4501/05 $50.00+.00

Available online at www.sciencedirect.com

SCIENCE DIRECT

Experimental Neurology 194 (2005) 203–211

Experimental Neurology

www.elsevier.com/locate/yexnr

Neuroprotective effect of oxidized galectin-1 in a transgenic mouse model of amyotrophic lateral sclerosis

Ren Chang-Hong[a], Manabu Wada[a,*], Shingo Koyama[a], Hideki Kimura[a], Shigeki Arawaka[a], Toru Kawanami[a], Keiji Kurita[a], Toshihiko Kadoya[b], Masashi Aoki[c], Yasuto Itoyama[c], Takeo Kato[a]

[a]*Department of Neurology, Hematology, Metabolism, Endocrinology and Diabetology, Yamagata University School of Medicine, 2-2-2 Iida-Nishi, Yamagata 990-9585, Japan*

[b]*Pharmaceutical Research Laboratory, Kirin Brewery Company, Ltd., Takasaki, Japan*

[c]*Department of Neurology, Tohoku University School of Medicine, Sendai, Japan*

Received 28 August 2004; revised 17 February 2005; accepted 19 February 2005
Available online 1 April 2005

Abstract

Abnormal accumulation of neurofilaments in motor neurons is a characteristic pathological finding in amyotrophic lateral sclerosis (ALS). Recently, we revealed that galectin-1, whose oxidized form has axonal regeneration-enhancing activity, accumulates in the neurofilamentous lesions in ALS. To investigate whether oxidized galectin-1 has a beneficial effect on ALS, oxidized recombinant human galectin-1 (rhGAL-1/ox) or physiological saline was injected into the left gastrocnemius muscle of the transgenic mice over-expressing a mutant copper/zinc superoxide dismutase (SOD1) with a substitution of histidine to arginine at position 46 (H46R SOD1). The H46R SOD1 transgenic mice, which represented a new animal model of familial ALS, were subsequently assessed for their disease onset, life span, duration of illness, and motor function. Furthermore, the number of remaining large anterior horn cells of spinal cords was also compared between the two groups. The results showed that administration of rhGAL-1/ox to the mice delayed the onset of their disease and prolonged the life of the mice and the duration of their illness. Motor function, as evaluated by a Rotarod performance, was improved in rhGAL-1/ox-treated mice. Significantly more anterior horn neurons of the lumbar and cervical cords were preserved in the mice injected with rhGAL-1/ox than in those injected with physiological saline. The study suggests that rhGAL-1/ox administration could be a new therapeutic strategy for ALS.

Keywords: Amyotrophic lateral sclerosis; Oxidized galectin-1; Cu/Zn superoxide dismutase; Transgenic mice

Introduction

Amyotrophic lateral sclerosis (ALS) is a fatal neurodegenerative disease characterized by loss of motor neurons in the cerebral motor cortex, brainstem, and spinal cord. ALS shows progressive muscle weakness and atrophy, with most patients dying within 5 years of disease onset (Cleveland, 1999; Rowland and Schneider, 2001). Usually, ALS occurs sporadically; however, approximately 10% of ALS cases show an autosomal dominant inheritance. Of these patients with familial ALS (FALS), 10–20% have missense mutations or a small deletion of the gene encoding Cu/Zn superoxide dismutase (SOD1) (Cleveland, 1999; Rowland and Schneider, 2001). Several lines of transgenic (Tg) mice with a FALS-linked mutated SOD1 gene have been made, and these mice have developed an adult onset paralytic disorder that is similar to sporadic and familial ALS (Bruijn et al., 1998; Gurney et al., 1994; Ripps et al., 1995; Tu et al., 1996). Accordingly, those Tg mice with SOD1 mutations have been used as an animal model for ALS.

Immunohistochemical investigations of the ALS spinal cord have shown that an abnormal accumulation of neuro-

* Corresponding author. Fax: +81 23 628 5318.
E-mail address: mwada@yacht.ocn.ne.jp (M. Wada).

0014-4886/$ - see front matter © 2005 Elsevier Inc. All rights reserved.
doi:10.1016/j.expneurol.2005.02.011

filaments in the cytoplasm and cell processes is a common pathological hallmark of both sporadic and familial ALS (Cleveland, 1999). The abnormal accumulation of neurofilaments induces axonal spheroids, cord-like neurite swellings, and perikaryal conglomerate inclusions in degenerating motor neurons of the spinal cord. These pathological features are considered to be important early pathological changes in ALS (Hirano et al., 1984; Kato et al., 2001). Therefore, an investigation of the accumulation of neurofilaments may help to understand the pathogenesis of motor neuron degeneration in ALS.

We have previously reported that galectin-1, which is a member of the β (beta)-galactoside-binding lectins, is accumulated in neurofilamentous lesions of the spinal cord in both sporadic and familial ALS (Kato et al., 2001). Galectin-1 has been shown to take two molecular forms: oxidized and reduced (Inagaki et al., 2000). Since oxidized galectin-1 has been reported to promote axonal regeneration after a peripheral nerve injury (Fukaya et al., 2003; Horie and Kadoya, 2000; Horie et al., 1999; Inagaki et al., 2000), it is possible that oxidized galectin-1 promotes the survival of the degenerating motor neurons in ALS.

The Tg mice expressing mutant human SOD1 with a substitution of histidine to arginine at position 46 (H46R SOD1) were established as a new animal model of familial ALS. In the present investigation, we administered oxidized galectin-1 to the H46R SOD1 Tg mice and subsequently assessed their disease onset, life span, duration of illness, and motor function. The present study showed that oxidized galectin-1 had a beneficial effect on the motor function and survival of Tg mice. This is the first report of a possible therapeutic effect of oxidized galectin-1 on ALS.

Materials and methods

Construction of transgenic (Tg) mice expressing mutant human SOD1

The present study was performed on Tg mice expressing mutant human SOD1 with a substitution of histidine to arginine at position 46 (H46R SOD1). We isolated a clone containing the full genomic human SOD1 gene, which was identified by screening a human genomic PAC library (Ioannou et al., 1994) using PCR with pairs specific to the human SOD1 gene. Subsequently, we cloned an 11.5 kb *Eco*RI–*Bam*HI fragment that contained the entire coding sequence and promoter region of the human SOD1 gene (Elroy-Stein et al., 1986; Levanon et al., 1985). The H46R mutation was engineered into this fragment by site-directed mutagenesis (Mutan-express Km, Takara, Otsu, Japan). The mutagenic primer and selection primer, which restored the Km resistance, hybridized to the vector and were incorporated during replication. The resulting potential Km resistant clone was subsequently sequenced (oligonucleotide-directed dual amber method) (Hashimoto-Gotoh et al., 1995) to verify the presence of either of the introduced mutations.

A linear 11.5 kb *Eco*RI–*Bam*HI fragment containing the H46R mutation was microinjected into BDF1 (C57BL/6 × DBA/2 F1) mouse (Jackson Laboratories, Bar Harbor, ME) embryos. The treated embryos were subsequently transferred to the oviducts of pseudopregnant ICR-scl female mice. The male littermates that were heterozygous for the H46R SOD1 mutation were used in this study. The mutated H46R SOD1 gene was identified by tail-clip PCR amplification using human SOD1-specific primers (sense primer: 5′-TTGGGAGGAGGTAGTGATTA-3′ and anti-sense primer: 5′-AGCTAGCAGGATAACAGATGA-3′). PCR was conducted with 1 cycle at 94°C for 2 min followed by 25 cycles at 94°C for 30 s, 58°C for 30 s, and 72°C for 30 s. Founder mice were then mated with C57B/6 mice (Jackson Laboratories).

Histopathological and immunohistochemical analysis

The mice were anesthetized with diethyl ether and killed by transcardiac perfusion with physiological saline followed by 4% paraformaldehyde containing phosphate-buffered saline (PBS; pH 7.4). The spinal cord was removed, post-fixed in the above solution, and embedded in paraffin. Serial transverse sections (4 μm thickness) of the lumbar segment (L_{4-5}) were cut and stained with hematoxylin and eosin (H&E) for a routine histological investigation. Several sections were also used for immunohistochemical investigations. Immunohistochemistry was performed using antibodies against human SOD1 (dilution 1:500, MBL, Japan), ubiquitin (dilution 1:100, DAKO, Denmark), and glial fibrillary acidic protein (GFAP; dilution 1:500, DAKO, Denmark). Deparaffinized sections were incubated with 1% H_2O_2 in distilled water for 10 min followed by 5% normal goat serum. The sections were subsequently incubated with primary antibodies in PBS containing 0.03% Triton X-100 at 4°C for 48 h. They were then incubated with a biotinylated secondary antibody (Vector, Burlingame, CA) for 2 h. After incubation with the avidin–biotin–peroxidase complex (ABC; Vector) for 1 h, peroxidase labeling was visualized by incubating the sections with 0.05 M Tris-buffered saline containing 0.05% 3,3′-diaminobenzidine tetrahydrochloride (DAB), 0.05 M imidazole, and 0.00015% H_2O_2 to yield a brown reaction product. The sections were then counter-stained with hematoxylin. Non-Tg mice were used for a comparison of histological findings.

Preparation of oxidized recombinant human galectin-1 (rhGAL-1/ox)

rhGAL-1/ox was obtained according to previous methods (Inagaki et al., 2000). In brief, rhGAL-1 was expressed in *Escherichia coli* and purified from the supernatant of the sonicated *E. coli* by DEAE-HPLC. Oxidized galectin-1

was obtained from bacterially expressed rhGAL-1 by the air oxidation method with $CuSO_4$ as a catalyst. DEAE-purified rhGAL-1 was subsequently diluted 20-fold with 20 mM Tris–HCl, pH 8.0, $CuSO_4$ was added to a final concentration of 0.0001% (w/v), and the mixture was maintained overnight at 4°C to allow disulfide bound formation.

rhGAL-1/ox was then purified by reversed-phase HPLC on a YMC-pack Protein RP column (YMC) with a linear gradient of acetonitrile in 0.1% trifluoroacetic acid. The purified rhGAL-1/ox contains three intramolecular disulfide linkages between Cys^2 and Cys^{130}, Cys^{16} and Cys^{88}, and Cys^{42} and Cys^{60}, which represent a stable conformation of oxidized galectin-1. Analysis by SDS-PAGE and HPLC revealed that rhGAL-1/ox was not degenerated even after 10 days of incubation at 37°C in PBS (5 μl protein/ml). rhGAL-1/ox confirmed that the protein promotes axonal regeneration in both the in vitro examination (Horie et al., 2004) and in the in vivo acellular nerve regeneration model (Fukaya et al., 2003).

Experimental protocol

Kadoya et al. recently reported that the application of rhGAL-1/ox (0.125 μg/body weight (g)/week) to the injured region promotes the restoration of nerve function using in vivo peripheral nerve regeneration model (Kadoya et al., in press). No one showed any toxic effects in reaction to the administration of rhGAL-1/ox. The concentration of rhGAL-1/ox in the present study was chosen because previous investigation demonstrated the effect and safety in an animal model and because a higher dose would be expected to promote the survival of the degenerating motor neurons. For the reasons above, 0.25 μg/g (body weight)/week of rhGAL-1/ox was administered to the H46R SOD1 Tg mice. Furthermore, intramuscular administration of rhGAL-1/ox was performed on a weekly basis in considering the application of rhGAL-1/ox to human ALS in the future.

The Tg mouse littermates were randomly divided into two groups: (1) administration of rhGAL-1/ox of 0.25 μg/g (body weight) (gal-1-treated group); and (2) administration of 60 μl physiological saline (control group). rhGAL-1/ox was diluted with physiological saline and injected into the left gastrocnemius muscle using a microsyringe connected to a 27-gauge needle. The control group received physiological saline instead of rhGAL-1/ox. To clarify whether rhGAL-1/ox delays the onset of the disease, intramuscular injection was started prior to the early presymptomatic stage. At postnatal day 70 (10 weeks of age), the mice started receiving a weekly intramuscular injection of rhGAL-1/ox or physiological saline. Twenty-eight transgenic mice (gal-1-treated group, $n = 14$; control group, $n = 14$) were used for the assessment of disease onset, life span, and duration of illness. Among them, 19 transgenic mice (gal-1-treated group, $n = 10$; control group, $n = 9$) were used for the assessment of motor function. Additional transgenic mice (gal-1-treated group, $n = 6$; control group, $n = 5$) were used for the histological and pathological investigation.

Assessment of motor function

Motor function was assessed using a Rotarod (Muromachi Instruments, Tokyo, Japan) on a weekly basis. The period for which a mouse could remain on a rotating axle (diameter, 30 mm; two sets of rotation speed, 5 and 20 rpm) without falling was measured. The time was automatically stopped if the mouse fell from the rod or after an arbitrary limit of 420 s (Li et al., 2000). Mice were tested once a week until they could no longer perform the task. An examiner who was blinded to the experimental design assessed the motor functions of the mice mentioned above. The onset of motor dysfunction was defined as the first day when a mouse could not remain on the Rotarod for 420 s at a speed of 20 rpm, as described previously (Li et al., 2000). The life span was defined as the postnatal day when the mouse died (Shefner et al., 2001). The duration of illness was defined as the number of days from the onset of motor dysfunction to death (Wang et al., 2002).

Assessment of body weights with transgenic mice

The body weight of each transgenic mouse was assessed on a weekly basis. Twenty-eight transgenic mice (gal-1-treated group, $n = 14$; control group, $n = 14$), which were used for the assessment of survival, were also used for the assessment of body weights.

Histopathological examination: tissue preparation and cell counting

The mice, which had been anesthetized with diethyl ether, were sacrificed by transcardiac perfusion with physiological saline followed by 4% paraformaldehyde containing PBS (pH 7.4). The spinal cord was removed, post-fixed in the above solution, and embedded in paraffin. Serial transverse sections (4 μm thickness) of the lumbar segment (L_{4-5}) were cut and stained with H&E for a routine histological investigation.

The number of spinal anterior horn neurons was examined at postnatal day 147 (21 weeks of age). Thirty serial sections each (10 μm thickness) of the cervical (C_{5-6}) and the lumbar cords (L_{4-5}) were stained by the Nissl method and photographed under light microscopy at 40× magnification. An examiner who was blinded to the experimental design counted the anterior horn cells that met all of the following criteria: (1) neurons located in the anterior horn ventral to the line tangential to the ventral tip of the central canal; (2) neurons with a maximum diameter of 20 μm or more; and (3) neurons with a distinct nucleolus (Manabe et al., 2003; Warita et al., 1999).

Statistical analysis

For the two groups, the disease onset, length of survival, and duration of illness were evaluated using the Log-rank. The results of motor function tested with the Rotarod and the body weights of transgenic mice were statistically analyzed using ANOVA for multiple comparisons among the groups. The number of anterior horn neurons in each group was compared using the two-tailed Student's t test. Statistical analysis was performed using computerized software (SPSS ver. 11.0, Chicago, Illinois, USA). $P < 0.05$ was accepted as statistically significant.

The experiment was approved by the Committee on Ethics of Animal Experiments and followed the Yamagata University School of Medicine Guidelines for Animal Experiments.

Results

Clinical phenotype and course of the transgenic mice

All the mice used had H46R mutant SOD1, as demonstrated by tail-clip PCR. These mice presented motor dysfunction similar to human ALS; the first sign of disease was weakness in their hind limbs, mostly shown by dragging of one limb. As the disease progressed, the mice showed marked muscle wasting in their limbs. The other muscles also became weak; thereafter, the affected mice could not move to reach their water supply and died. The motor dysfunction occurred at about 20 weeks of age, and most mice died at about 24 weeks of age.

Histopathological and immunohistochemical studies in the spinal cords

In mice at the early presymptomatic stage (91 days of age), no apparent changes were observed in the H&E-stained sections (Fig. 1A). Small numbers of GFAP-immunoreactive astrocytes were seen (Fig. 1E). At the late presymptomatic stage (119 days of age), large anterior horn cells seemed to decrease in number (Fig. 1B). By 147 days of age (the early symptomatic stage), when weakness of the limbs became apparent, there was a marked loss in the number of anterior horn cells (Fig. 1C) accompanied by astrocytic proliferation (Fig. 1G). Neurite swellings in the anterior horns were also observed (Fig. 2B). Eosinophilic inclusion bodies similar to Lewy body-like hyaline inclusions in human ALS were detectable in the anterior horns. These inclusions were immunostained with anti-SOD1 antibody and anti-ubiquitin antibody, most of which were detected in the neuropil (Figs. 2A and C), and only a few were within the perikarya of neurons (Fig. 2D). At the end stage, there was a severe decrease in the number of anterior horn neurons (Fig. 1D) with diffuse astrocytic proliferation (Fig. 1H). There were no remarkable vacuoles like those in cell bodies, dendrites, and axons of previously reported transgenic mice expressing SOD1 mutation G37R (Wong et al., 1995) or G93A (Gurney et al., 1994).

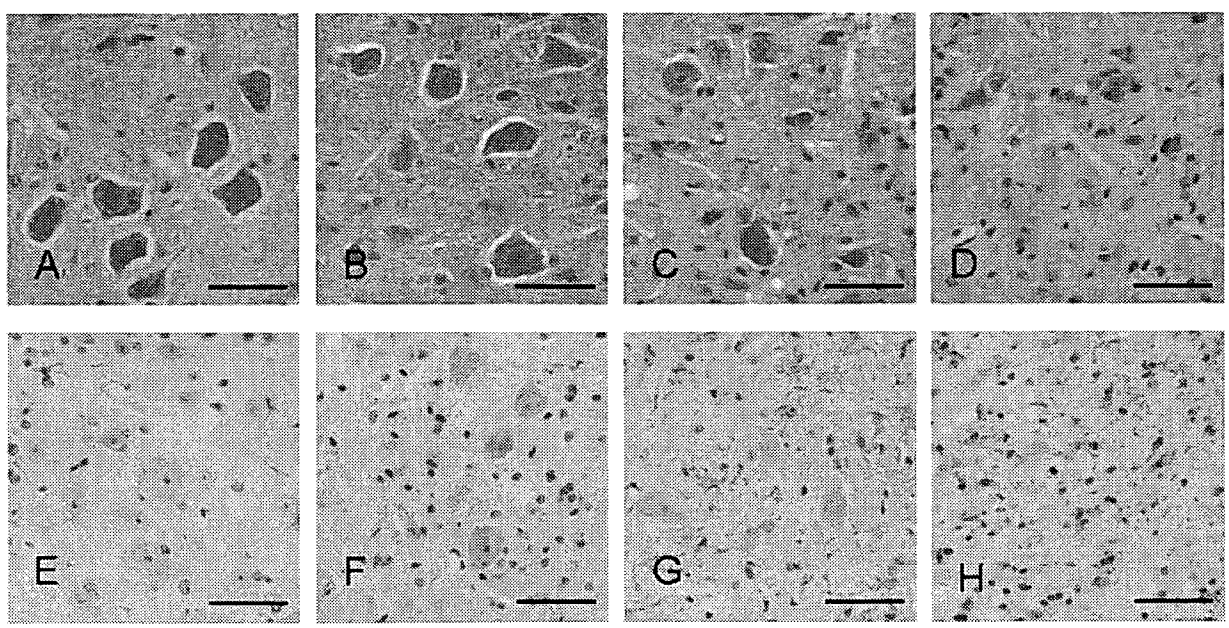

Fig. 1. Histopathological findings of the lumbar cord in the H46R transgenic mice. Sections were stained with hematoxylin–eosin (H&E) (A–D) and immunostained with anti-glial fibrillary acidic protein (GFAP) antibody (E–H). (A, E) No apparent changes are observed in the section stained with H&E in the early presymptomatic stage (91 days of age). Small numbers of GFAP-immunoreactive astrocytes are seen. (B, F) The number of large anterior horn cells seems to decrease in the late presymptomatic stage (119 days of age) accompanied by astrocytic proliferation. (C, G) A marked loss of anterior horn cells is seen with an increase in the number of astrocytes at the early symptomatic stage (147 days of age). (D, H) A severe loss of anterior horn neurons is observed at the end stage (168 days of age). Scale bars = 50 μm.

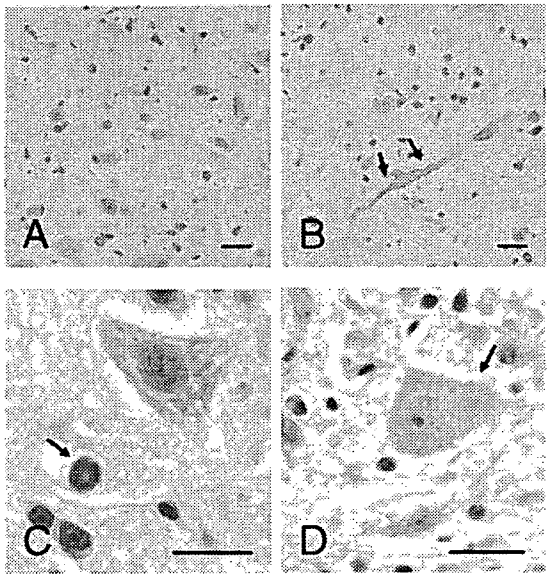

Fig. 2. (A) Many inclusion bodies, immunostained with anti-ubiquitin antibody, are readily apparent in the neuropil of the spinal ventral horn. (B) Cord-like neurite thickening of the ventral horn is immunostained with anti-ubiquitin antibody. (C) A Lewy body-like inclusion in neuropil is immunostained with anti-ubiquitin antibody. (D) A Lewy body-like inclusion immunostained with anti-SOD1 antibody is seen in the spinal anterior horn neuron. Scale bars = 20 μm.

Effects of rhGAL-1/ox on the disease course

rhGAL-1/ox delayed the onset of disease

The onset of the disease, as defined by falling from the Rotarod (20 rpm) within 420 s, occurred at postnatal day 138.3 ± 1.7 in the control group. The gal-1-treated mice showed a statistically significant delay of onset (postnatal day 143.5 ± 1.5) (P = 0.0156) (Fig. 3A and Table 1).

rhGAL-1/ox prolonged survival

The life span was much longer (172.2 ± 1.3 days) in the mice in the gal-1-treated group than in those in the control group (160.4 ± 2.4 days) (P < 0.0001) (Fig. 3B and Table 1).

rhGAL-1/ox prolonged the duration of illness

The duration of illness was significantly longer in the mice in the gal-1-treated group (28.7 ± 1.8 days) than in those in the control group (22.1 ± 1.4 days) (P = 0.0072) (Table 1).

rhGAL-1/ox improved motor function

In the condition with 5 rpm, which was a weak task, differences in motor function between the two groups were not apparent at postnatal day 133 (19 weeks of age). Although motor function appeared to be better in the mice in the gal-1-treated group than in those in the control group at the early symptomatic stage, the difference between two groups was not statistically significant (ANOVA; P = 0.282) (Fig. 4A).

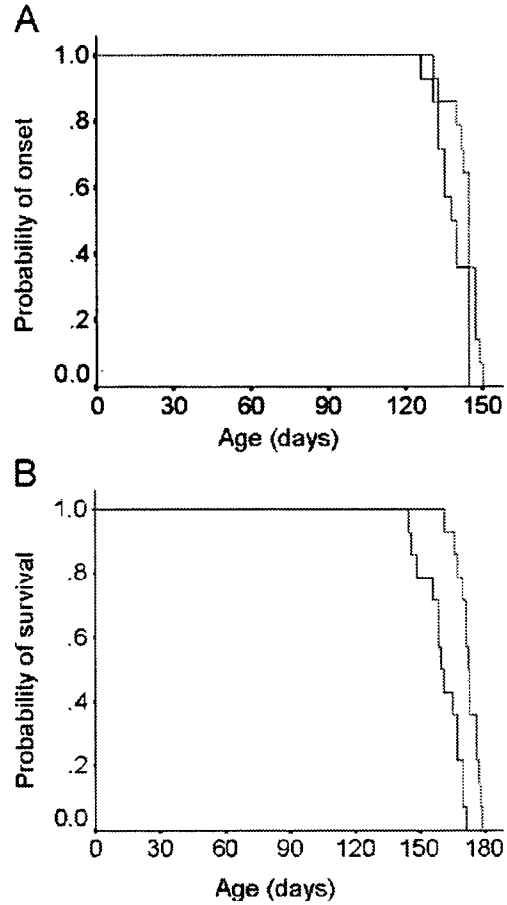

Fig. 3. rhGAL-1/ox delayed the disease onset and prolonged the survival of Tg mice (mutant H46R SOD1). The Kaplan–Meier curves demonstrate the probability of onset of Rotarod deficit (A) and length of survival (B) in Tg mice (mutant H46R SOD1). The onset of the Rotarod deficit was more delayed in the gal-1-treated group than it was in the control group (P = 0.0156) (A). The life span was significantly more prolonged in the gal-1-treated group than in the control group (P < 0.0001) (B). Red line, gal-1 group (n = 14); blue line, control group (n = 14).

In the condition with 20 rpm, which corresponded to a heavy task, motor function was better in the gal-1-treated mice than in the control group mice at postnatal day 103 (19 weeks of age). The motor function of the mice in the gal-1-treated group was significantly better than that in the mice in the control group (P = 0.038) (Fig. 4B).

The body weight changes of the transgenic mice

At the end stage (168 days of age), the mice in the control group showed a body weight loss by 7%, compared

Table 1
Onset of motor dysfunction, survival, and duration of illness

	Control (n = 14)	Gal-1 (n = 14)	P value
Onset (postnatal days)	138.3 ± 1.7	143.5 ± 1.5	0.0156
Survival (days)	160.4 ± 2.4	172.2 ± 1.3	<0.0001
Duration (days)	22.1 ± 1.4	28.7 ± 1.8	0.0072

Values tabulated are mean ± SEM. Statistical comparisons were with Log-rank test.